Arab J Geosci (2015) 8:11049–11072
DOI 10.1007/s12517-015-1966-5

ORIGINAL PAPER

Geological evolution of Nile Valley, west Sohag, Upper Egypt: a geotechnical perception

El-Sayed Sedek Abu Seif[1,2]

Received: 16 December 2014 / Accepted: 21 May 2015 / Published online: 30 May 2015

Abstract Based on distinct variations of textural characteristics, stratigraphical relationships and mineral composition of clastics sedimentary sequence (coarse aggregates) in west Sohag, Upper Egypt had been classified into six individual geological evolutionary stages. These stages were controlled mainly by geomorphology, paleo-climatic conditions, and regional and local tectonic events. In west Sohag, Upper Egypt, the suitability of the Oligocene–Pleistocene natural coarse aggregates have been examined in terms of pavement materials in a sub-base consideration. Depending on textual characteristics and mineral composition, these natural coarse aggregates indicated three distinct stages of geological evolution of the Egyptian Nile Valley. These aggregates are classified as well-graded gravels (GW) and distinguished by cubical shape with sub-angular to sub-rounded edges, as well as characterized by a relatively high abrasion resistance. This leads to a suitability of these natural aggregates in being used as a sub-base pavement course for higher shear strength, exhibiting a less fatigue life. The total estimated volume of these coarse aggregate is 2060.41 million m^3. This volume of natural coarse aggregates can be dry sieved and crushed to produce base and surface pavement courses.

Keywords Natural coarse aggregates · Textural characteristics · Sub-base course · Nile Valley · Upper Egypt

✉ El-Sayed Sedek Abu Seif
esmansor@kau.edu.sa; elsayed_71@Yahoo.com

1 Faculty of Earth Sciences, King Abdul Aziz University, Jeddah, Saudi Arabia

2 Geology Department, Faculty of Science, Sohag University, P.O. Box 82524, Sohag, Egypt

Introduction

The geological evolution of sedimentary rock units of the studied area (Sohag Governorate, Upper Egypt) can be considered as a thumbnail of the geological evolution of the Nile Valley especially in the period ranging from Post-Eocene to recent. The evolution of the geological history in the study area has been influenced mainly by paleo-climate, local and regional tectonics, and paleo-geomorphology. Climatic indicators point to a cyclic climatic evolution from humid, semi-arid to arid conditions. The depositional features as well as mineral composition and aerial distribution of Post-Eocene clastic sedimentary sequence (coarse aggregates) in the studied area had been controlled mainly by these cyclic paleo-climatic conditions and tectonic events.

Aggregates represent a very important and effective component of all construction materials, so that, it is essential to evaluate the main effective characteristics of these aggregates through standard tests. Frequently, the rock units in the Egyptian Nile Valley nearly are consisting of sedimentary rocks. So in the non-basement complex areas the pavement materials with high quality can be rarely found to use as natural material and the crushed aggregates are more expensive than natural materials. The material used at the sub-base layer must be selected as transport of traffic load and upper layers weight.

In Upper Egypt, natural aggregates are widely distributed with a huge range of potential sources. They are of low-cost products and play an effective role in the growth of the Egyptian economy. The suitability of aggregates to be used in asphaltic mixtures depends on their physical, mechanical, and mineralogical properties. These properties primarily control the performance of mixtures. In recent decades, the growth in industrial production and consequent increase in consumption has led to a fast decrease of available natural resources (raw materials or energy sources). More than 95 % of asphalt pavement materials (by weight) consist of aggregates. The highway and construction industries consume a huge amount of aggregates annually causing considerable energy and environmental losses. The aggregates are usually produced from neighborhood aggregate quarries or from natural aggregate sources (Akbulut and G rer 2007).

In Sohag Governorate (Upper Egypt), the natural coarse aggregates are broadly distributed with a considerable thickness especially in western side of the Nile Valley and represented an important source of aggregate materials. Little attention has been given to the geotechnical characteristics of these aggregates. This study aims to investigate the geological characteristics of the Oligocene (?)–Pleistocene coarse aggregates in order to evaluate these aggregates as natural pavement aggregates.

Geological setting

The area under investigation represents a part of the Nile Valley of Upper Egypt. It extends between latitudes 26° 00′ and 26° 30′ N and longitudes 31° 30′ and 32° 00′ E. The geology of the studied area can be summarized as follows (Fig. 1):

1. The Nile Valley in the studied area is bounded by the lower Eocene limestone plateaus. Due to variations in the lithology and faunal content, this sequence is divided into two formations; the Thebes Formation at the base and the Drunka Formation at the top.

    a. The Thebes Formation (Lower Eocene, was first introduced by Said 1990) is represented by a thick bedded and laminated limestone succession with flint bands. Lithologically, the lower part of the Thebes Formation is characterized by a medium- to thick-bedded, massive yellowish white limestone with abundant Nummulites, Assilines, and Operculines (Mahran et al. 2013).
    b. The Drunka Formation covers more than 90 % of the area around Sohag. It overlies the Thebes Formation and is easily differentiated from it by its snow white color and massive bedding. The Drunka Formation is composed of a laminated limestone with chert bands interbedded with bioturbated hard massive limestone, including large silicified limestone concretions (up to 1.2 m in diameter). The upper part (up to 100 m) is composed of a grayish white, massive to bedded bioturbated limestone (Mahran et al. 2013).

3. The Katkut Formation (Pre-Eonile, Late Oligocene?) was firstly introduced to the Post-Eocene stratigraphy of the west side of the Nile Valley by Issawi et al. (1999) and Issawi (2005). The Katkut Formation unconformably overlies the Early Eocene sequence. It is considered as the oldest coarse aggregate in the studied area. The type section of the Katkut Formation is located at the southern flank of Wadi El-Yatim (Figs. 1 and 4).
4. The Abu Retag Formation (Late Miocene sequence?)—the formal name Abu Retag Formation has been newly introduced to the local stratigraphy of the Nile sediments by Mahran et al. (2013) to describe the mottled reddish brown coarse aggregates sequence that predominantly crop out along the lower slopes of the western Eocene limestone scarps (Fig. 1).
5. The Issawia Formation (Early Pleistocene, Said 1981; Mahran 1992) is composed of a massive rubble breccias succession topped by characteristic hard red breccias. The Issawia Formation crops out along the margins of the Eocene escarpment. It is represented by inclined beds of hard red breccias (up to 15 m thick).
6. The Armant Formation according to Said (1975, 1981) consists mainly of fine conglomerate beds alternating with bedded travertine carbonates.
7. The Qena Formation (Said 1981) is formed from a thick succession dominantly by fine aggregates filling low-topographic hills with rounded surfaces and low scarps extending in NW-SE direction near to the cultivated land. In the northern part of the study area, many quarries are used to exploit the Qena Formation for construction purposes (Abu Seif 2014a).
8. The Abbassia Formation (Said 1975, 1981) consists of the gravel sequence overlying the Qena Sands. West of Sohag, the Abbassia Formation is 10 m thick, unconformably overlying the Armant Formation (e.g., Wadi El-Yatim, Wadi Dukhan; Figs. 1 and 4). Locally, these sediments are trapped in low-topographic areas west of Armant and Abu Retag formations (Fig. 1) and are dominated by progradational conglomerates which are laterally inter-fingering with sandstones and siltstones.
9. The Dandara Formation was first proposed by Said (1981) to describe the silt and fine-sand section west of Dandara (~100 km south of the study area). The Dandara Formation is generally closer to the cultivated land and is represented by sand and silt intercalations.
10. Flood Plain sediments (cultivated lands) are mainly restricted along the narrow tract of the River Nile Valley.
11. Recent Wadi deposits vary greatly in both thickness and texture depending on land morphology and intensity and regime of flashflood rainfall (Omran 2008).

Geological evolution of the studied area

The relative roles of tectonics and climate in shaping the Earth's landscape have received significant attention (Goudie 2005). The northernmost segment of the Nile River contains a record of over 20 Ma of geologic history displaying the

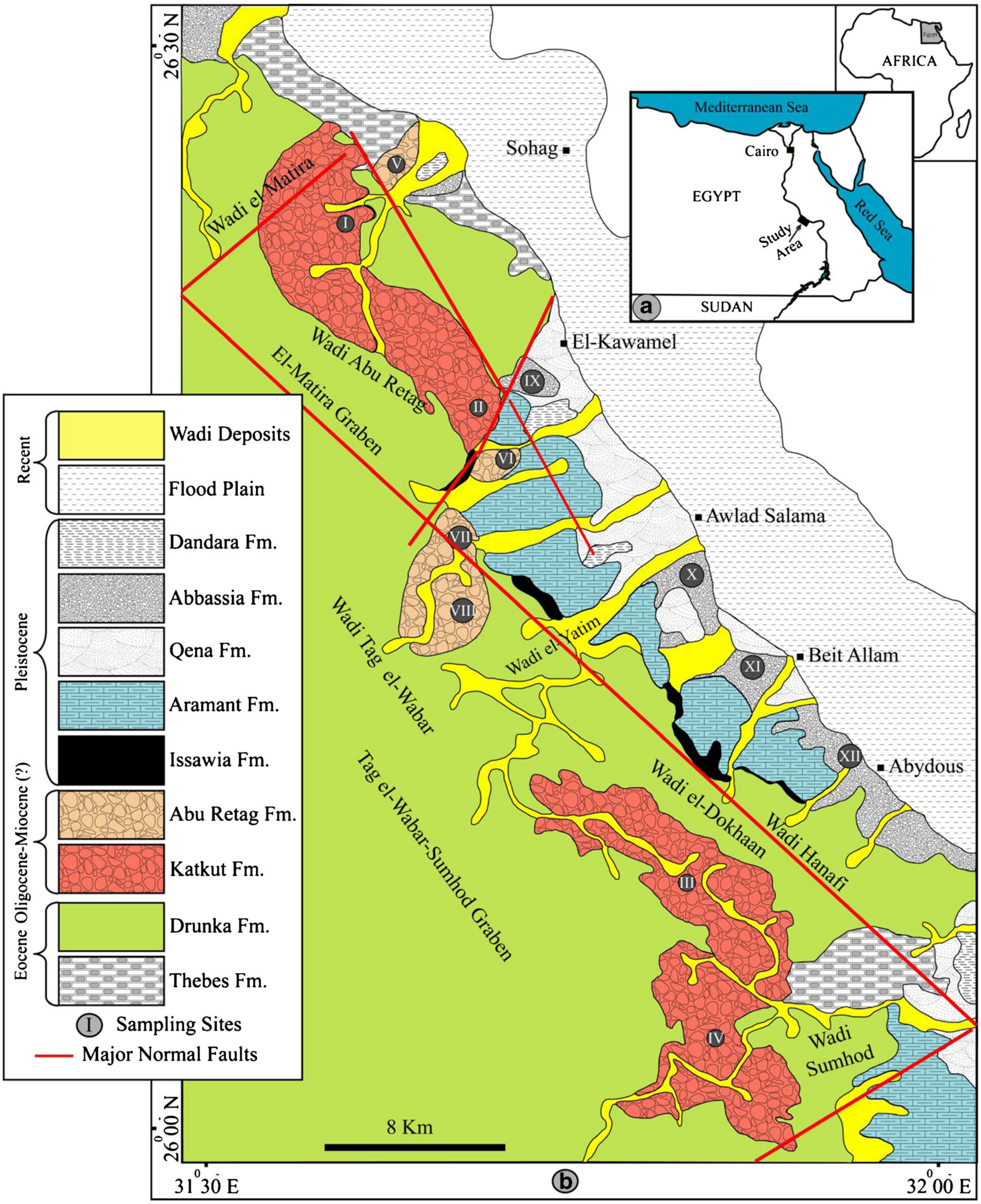

Fig. 1 Location map (*A*) and geological map (*B*) of west Sohag Governorate modified from Conoco (1987)

relationship between evolving drainage systems and regional tectonics (Roden et al. 2011). There are several factors affecting the distribution of the Post-Eocene sedimentary rock units in the Egyptian Nile Valley:

1. Regional tectonics, e.g., the opening of the Red Sea and associated uplifting of the Red Sea Hills (McCauley et al. 1986; Issawi and McCauley 1992, 1993; Issawi et al. 1999; Issawi and Osman 2008),
2. Local structures, e.g., the presence of Cretaceous and younger faulting (Akawy 2002; Thurmond et al. 2004), and
3. Climate changes, e.g., the Messinian Salinity Crisis and the emergence of the Sahara (Butzer 1959; Butzer and Hansen 1968; Wendorf and Schild 1976; Said 1993).

Based on distinct variation in lithology, stratigraphic relationships and mineral content Said (1981, 1983) discussed the geological history of the River Nile and proposed that the Egyptian Nile evolved through five stages including Eonile, Paleo-Nile, Protonile, Pre-Nile, and Neonile. The other six phases of the Egyptian Nile evolution include the Gulf phase, the Paleo-Nile phase, the Desert phase, the Pre-Nile phase, the Neonile phase, and the Modern Nile phase (Roden et al. 2011).

The northernmost segment of the Nile system is especially of great importance to understand the geological and geomorphological evolution that went through many phases which were influenced by geological events such as the uplift of the Red Sea, the Nubian swell, and the Messinian salinity crisis and emergency of Sahara (Said 1993).

The onset of the N-flowing Egyptian Nile is suggested to have started ~6 Ma ago with the Eonile phase where a 1000-km-long and 300–1000-m-deep canyon (Eonile canyon) was carved under the trace of the Modern Nile (Said 1993). This event was linked to the desiccation of the Mediterranean Sea, resulting in the lowering of the river's baseline and allowing for deep headword incision (Roden et al. 2011). Prior to the Eonile phase, in what is referred to here as the Pre-Eonile phase, numerous rivers flowed from the east across the Eastern Sahara originating from the uplifted terrain of the Red Sea Hills (Said 1993; Issawi and McCauley 1993; El-Bastawesy et al. 2010).

The studied area is dominated by NW-, N-, NE-, and ENE-trending faults and fractures; some of these fractures controlled the course of this part of the Nile Valley (Mahran et al. 2013). Six individual evolutionary stages of the Egyptian Nile in west Sohag were recognized (Fig. 2):

1. The Pre-Eonile stage had been represented by gravels and sandy gravels of the Katkut Formation (Late Oligocene–Early Miocene?). These gravelly sediments were filling the NW-trending grabens by stream flow-dominated alluvial fans and braided plains.
2. During the Eonile system, braided plains conglomerates of the Abu Retag Formation (Middle-Late Miocene?) developed in the hanging walls of the linked NW- and ENE-trending fault segments. The Eonile phase was controlled by the Messinian Salinity Crisis, when the desiccation of the Mediterranean Sea resulted in carving of a ~1000-km-long, ~300–1000-m-deep canyon stretching in a N–S direction from the Nile Delta to the City of Aswan (Said 1981, 1993; Issawi and McCauley 1992; Krijgsman et al. 1999; Roden et al. 2011).
3. The third-stage sediments were represented by a long series of interbeded brownish clays and thin fine-grained sand and silt laminae of the Madmoud Formation (Pliocene, Said 1981) which crop out along the banks of the valley and many of the wadis which drain in it. In the studied area, the Madmoud Formation is represented by a subsurface sequence and exposed with widely aerial distribution in east Sohag Governorate.
4. In the fourth stage, during the Protonile stage, the intersections of fault segments led to the development of local reentrants, which are later filled by siliciclastics and mixed siliciclastics-carbonates of Issawia and Armant formations. The advent of the Pleistocene epoch in Egypt was marked by dramatic events the most important of which being relative to their impact to climate and tectonisim.

During Early Pleistocene, the studied area was subjected to spring activity and deposition of bedded and/or massive tufas (Issawia Formation). These tufas are associated with thick talus red breccias which accumulated during an episode of high seismicity along the piedmont slopes of the bounding cliffs. The Isswia Formation is followed upward by pluvial coarse gravels (Aramant Formation, Said 1981). The gravels of the Aramant Formation seem to have been derived from deeply leached terrain and from

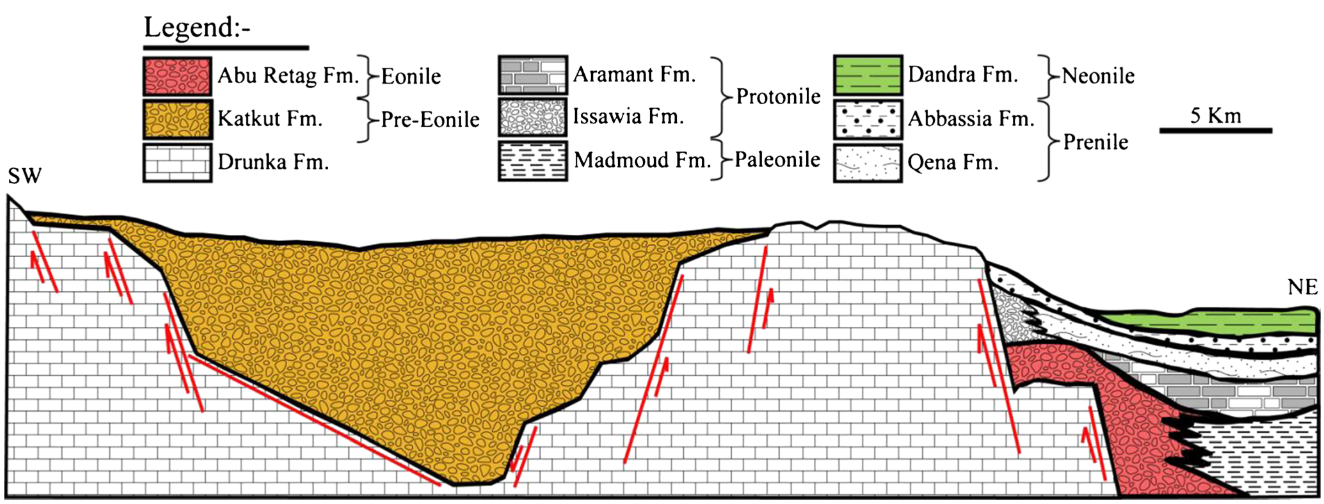

Fig. 2 SW-NE cross section showing the main lithostratigraphic units of Pre-Eonile-Neonile sedimentary rock units west of Sohag Governorate, Upper Egypt

local sources. Both Issawia and Armant formations are laterally inter-tonguing (Mahran 1992; Mahran et al. 2013).

5. During the fifth stage, the Protonile was succeeded by two other rivers, the Pre-Nile (Qena Formation, Said 1981) and the extant Neonile (Abbassia Formation). The sedimentary rock units of each river are distinct in lithology, stratigraphic relationships, and mineral content. They are separated from each other by an unconformity and long recession.

   The mineral composition of the Qena Formation indicates that the Egyptian Nile was connected for the first time with the Ethiopian highlands across the elevated Nubian massif by way of a series of cataracts.
6. In the final sixth stage (Neonile stage), the flooding of the new river over the low-topographic areas caused deposition of floodplain fine siliciclastics, alluvial conglomerates, and lacustrine carbonates of Dandara and cultivated land made up of clays, silts, and sands.

Stratigraphic relations and field observations

The studied coarse aggregates are characterized by absence of an index fossil, so that the integrated stratigrahical relations and field observations had been used to reconstruct an acceptable geological evolution of the studied area. Generally, these sediments are grouped into three main lithostratigraphic sequences; the Lower Eocene limestone sequence, the Late Oligocene–Late Miocene sequence (Pre-Eonile–Eonile), and the Pliocene–Quaternary sequence (Paleo-Nile–Neonile). Each sequence has distinct features in lithology and stratigraphic relationships and is limited by a clear structural discordance (Mahran et al. 2013).

Lower Eocene limestone sequence

In the studied area as a general case in Upper Egypt, the Nile Valley is bounded by the lower Eocene limestone plateaus where owing to variations in the lithology and faunal content, this sequence is divided into two rock units; the Thebes Formation at the base and the Drunka Formation at the top. In the study area, the Thebes Formation is locally distributed and represented by 30 m of laminated limestone enriched with flint bands west of El-Kawamil village, where it conformably underlies the Drunka Formation (Fig. 3). The Drunka Formation covers more than 90 % of the studied area. It is easily differentiated by its snow white color and massive bedding. The Drunka Formation is composed of laminated limestone with chert bands interbedded with bioturbated hard massive limestone, including large silicified limestone concretions (up to 1.2 m in diameter).

Late Oligocene–Late Miocene sequence (Pre-Eonile–Eonile)

The Katkut Formation (Pre-Eonile)

Here, the Katkut Formation name is used to describe all coarse clastic sediments (coarse natural aggregates) unconformably overlying the Early Eocene sequence (Figs. 1 and 4). These gravelly sediments were filling the Early Eocene sequence NW grabens (Issawi et al. 1999; Issawi 2005; Mahran et al. 2013); in the studied area, these grabens are represented by Wadi El-Matira graben and Wadi Tag el-Wabar-Sumhod graben (Fig. 1). The type section for the Katkut Formation is located at the southern flank of Wadi El-Yatim (Figs. 1 and 4) where it unconformably overlies the Drunka Formation and its basal part occurs as subsurface (Fig. 5a).

The coarse aggregates of the Katkut Formation begin at the base with scouring filled with boulder conglomerates then passes upward into 10–15-m-thick series of fining-upward cycles. Each cycle is separated by an erosive base varying in depth from 20 to 60 cm. The erosive bases between these cycles suggest that they were deposited by confined water flow (Hoggs 1982). An excellent example of these cycles is found at Wadi El-Yatim (Fig. 4).

Generally, the coarse aggregates of the Katkut Formation exhibit wedge-like geometry, well roundness, well textural maturity, erosive scour, and irregular surfaces. The gravels (coarse aggregates) of Katkut Formations are mainly composed of well-rounded clasts of chert and silicified limestone. These features indicate prolonged episodic abrasion, long transport distance, and rapid flow conditions. The presence of large blocks of nummulitic limestone of the Drunka Formation points to syndepositional tectonic activation along eastern and southeastern flanks of the graben. Its components are devoid of basement pebbles as will be discussed later.

Based on its depositional characteristics and erosional processes, the Katkut Formation can be subdivided into three unconformably bounded units. The lowermost unit consists of about 15 m thick of gravels and sandy gravels fining-upward cycles. The middle unit composed mainly of 25 m thick of mottled and reddish brown cross-bedded sands and silts. The uppermost unit (~15 m thick) consists mainly of well-packed tabular cross-bedded sandy gravels (Fig. 5b). The paleo-depositional current measurements using imbrication fabrics indicate N to NW flow directions (Fig. 5c). Also, syndepositional slumping, truncations, folding, and faulting are common (Fig. 5d).

These depositional as well as paleo-environmental characteristic features of the Katkut coarse aggregates concluded that the deposition occurred as stream flows to braided channel-dominated alluvial plain environments (Blair and McPhersonb 1994; Mahran et al. 2013). A debris to stream flow-dominated alluvial fans of the lower part of this

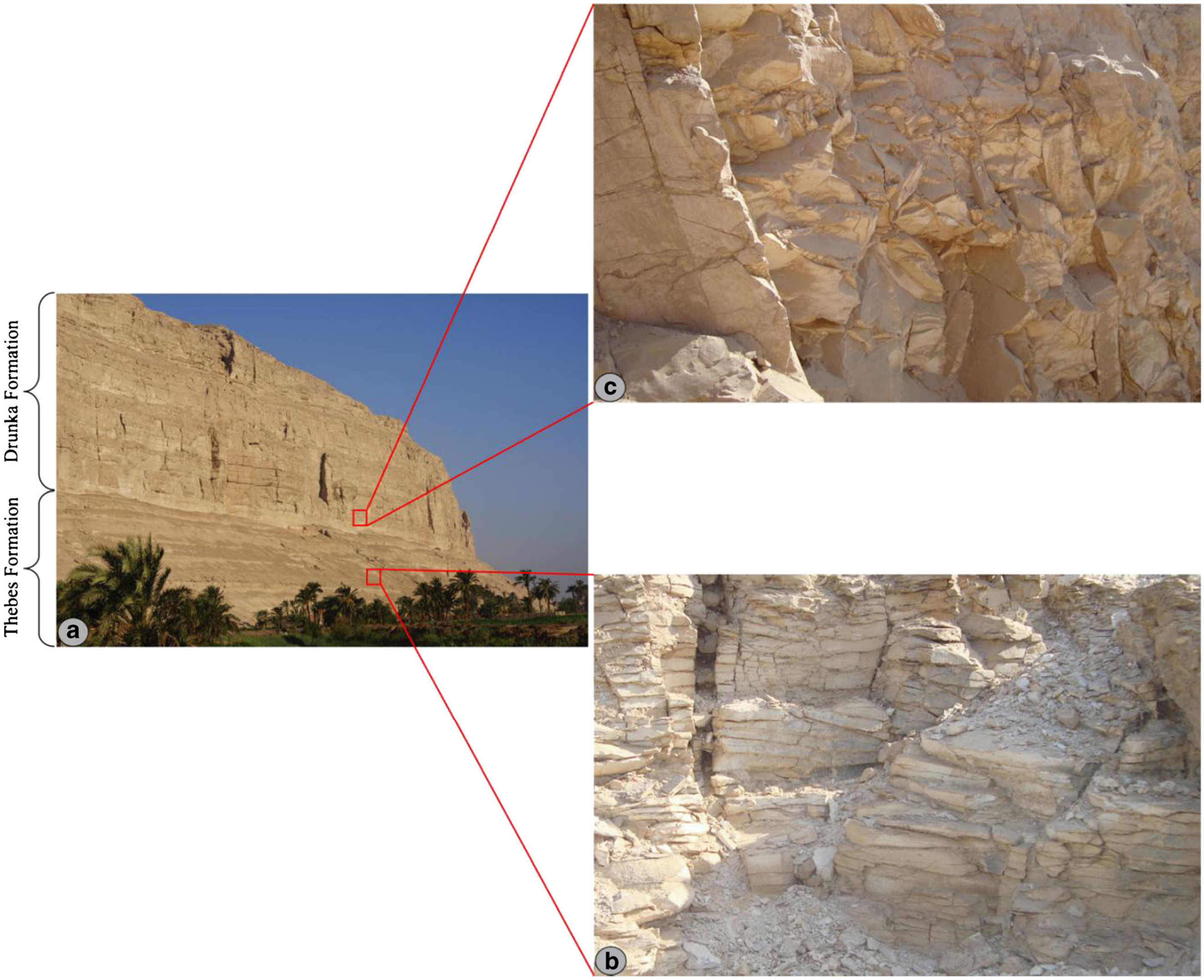

Fig. 3 Contact between Thebes and Drunka formations (**a**), laminated limestone enriched with flint bands of Thebes Formation (**b**), and snow white massive bedded and fractured limestone of Drunka Formation (**c**)

association suggested a lack of inverse grading and presence of outsize boulders, as well as crude stratification of the disorganized gravels and vertically oriented-long axis of the gravel particles (Fig. 5e, Dec 1992; Hadlari et al. 2006; Mahran et al. 2013).

This paleo-drainage system was just one of many W-flowing rivers sourced from the east by the Precambrian crystalline rocks of the Red Sea Hills, which were uplifted in association with the opening of the Red Sea. Fission track studies by Omar and Steckler (1995) suggested that the early stages of rifting in the Red Sea were characterized by two distinct episodes of uplift that occurred between ~34 (Oligocene) and 25–21 Ma (Miocene).

Consequently, the middle unit of the Katkut Formation is characterized by fining-upward mottled and reddish brown (massive, laminated, and cross-bedded) sand and silt cycles separated by paleosol horizons (Fig. 4). The silt-sized grains are predominantly sedimentarily structureless and characterized by yellow to reddish brown. These features point to low-energy-concentrated flow depositional environment (Amoroso et al. 2008; Mahran et al. 2013). Also, the sand-sized particles are characterized by a very good sorting, which may indicate reworking of aeolian sands (Mahran et al. 2013). These aeolian sands may be derived from surface-outcropped Cretaceous Nubian Sandstone from ancient rivers during past pluvial episodes during pre-uplifted Red Sea basement hills (Oligocene). Prior to the Eonile phase, paleo-drainage system indicated the presence of many flowing rivers sourced from the east (Roden et al. 2011). Flat depressions and drainage channels were developed during wetter climate Oligocene phases (El Aref et al. 1987; Kröpelin 1993). Structural and sedimentological studies indicated absence of any significant uplift and the dominance of low relief prior to the Miocene epoch (Bosworth et al. 2005; Roden et al. 2011).

Owing to absence of index fauna in both continental coarse and fine aggregates of Katkut Formation, as well as based on

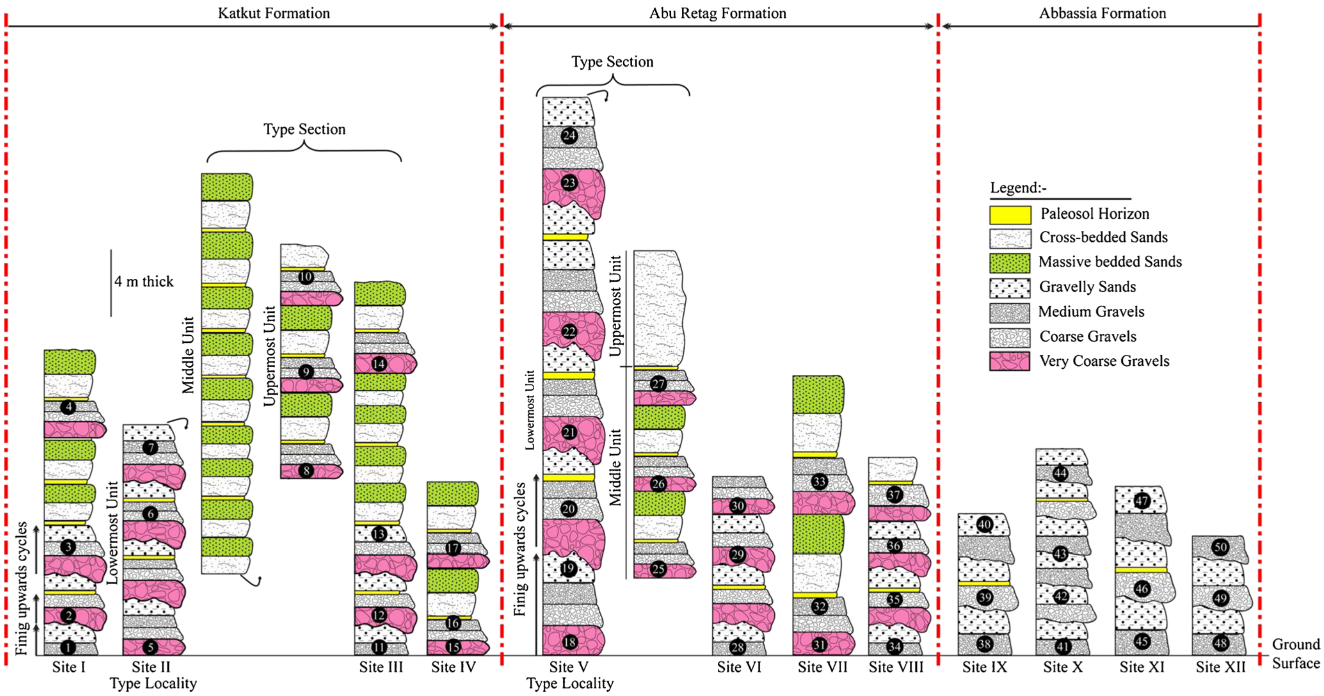

Fig. 4 Columnar sections and sample numbering of the studied natural coarse aggregates

stratigraphic position and field relations Katkut Formation assigned to late Oligocene–Early Miocene age. There are many indicators support this opinion as follows:

- The NW-trending fault grabens in which the sediments of the Katkut Formation were deposited, clearly deform the Eocene limestone so these graben-filled sediments must be younger than the Eocene age Mahran et al. (2013).
- The coarse gravels and sandy gravels of the Katkut Formation have very close resemblance in composition with that of well-known Late Oligocene conglomerates of Egypt, through the correlation with other and similar gravelly units in nearby areas. These gravels are analogous to the Late Oligocene Nakheil Formation on the eastern side of the Red Sea Mountains (Akkad and Dardir 1966; Mahran 1997, 1999).
- The coarse aggregates of the Katkut Formation are composed mainly of chert and silicified limestone and devoid of any Precambrian basement pebbles (Table 1; Fig. 10). The rare granitic and volcanic rocks in these deposits prove that the Precambrian Red Sea Mountains were not exposed during the early stages of the rift phase, which was started during Late Eocene–Early Oligocene time (Mahran et al. 2013). Brookes (1999, 2001) considers that the Cenozoic gravels spreading over Egypt's Western Desert are of fluvial origin and deposited in NW-trending major flutes that were possibly formed by catastrophic flood erosion by the end of Oligocene time.
- Toward the end of the Eocene time, on the eastern regions of Egypt, streams flowed westward down the slopes from doming in the region preceded rifting of the continent in Miocene time and deposited gravelly sediments from erosion and denudation of the emerging landscape of the flanking Red Sea region overlying the limestone plateau (Issawi and McCauley 1992). The streams of the Oligocene age contributed to widespread denudation of the region; deposits of fluvial sands, flint cobbles, and petrified wood are identified from this long humid episode (McCauley et al. 1982).
- The Katkut Formation can be stratigraphically correlated with Oligocene sequences in other similar area, e.g., in Quseir area, Nakhul Formation (Akkad and Dardir 1966; Abdel Razzik 1972; Said 1992; Mahran 1997, 1999) and Gebel Ahmar Formation (Barron 1907; Shukri 1954; Said 1962). In north of El-Fayoum Depression, Gebel Qatrani Formation (Beadnell 1905; Said 1962; Bown and Kraus 1988; Mandanici et al. 2010; Abdel Hamid et al. 2014), and Qatrani Formation at Widen El-Faras Hills (Shukri and Ayouty 1954; Said 1962).

The Abu Retag Formation (Eonile) The formal name Abu Retag Formation has been newly introduced to the local stratigrapgy of the Nile Valley sediments by Mahran et al. (2013) to describe the mottled reddish brown coarse clastic sediments that predominantly crop out along the lower slopes of the western Eocene limestone scarps (Fig. 6). The Abu

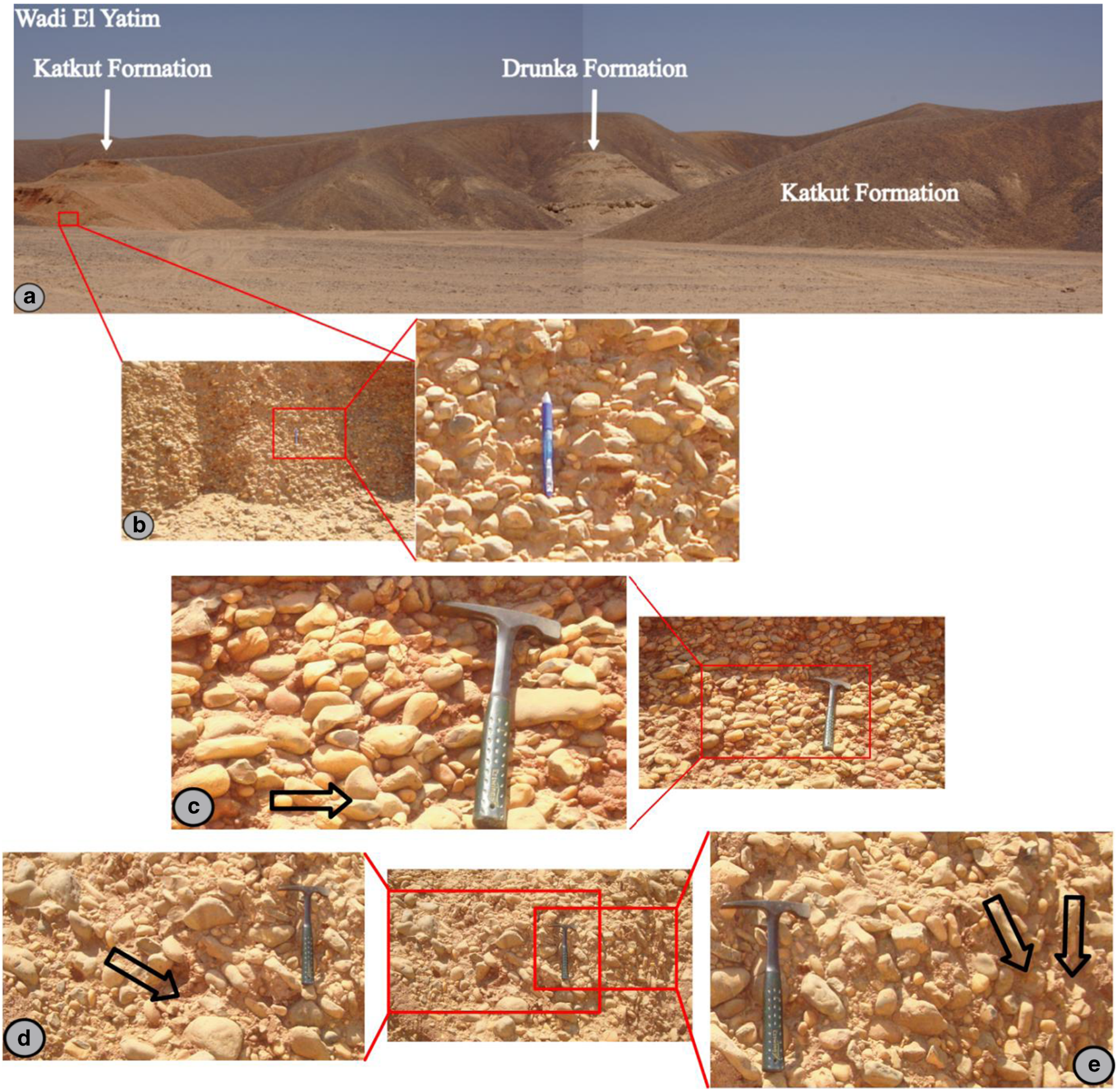

Fig. 5 Field photographs showing natural coarse aggregates of Katkut Formation unconformably overlies Drunka Formation (**a**) as well as its depositional characteristic features (**b**–**e**)

Retag Formation is considered the first stage of fluvial sedimentation within the Nile basin fill (Mahran et al. 2013). Its type locality as well as type section has been measured at the northern flank of Wadi Abu Retag (Figs. 4 and 6a) where its thickness is about 50 m.

Mostly, the sequence of Abu Retag Formation exhibits wide range texturally and compositionally. It was well developed in the hanging wall of the NW, N, and NE fault segments, where Eocene plateau is intensely faulted. Locally, the Abu Retag Formation unconformably overlies the tilted carbonate blocks of the Drunka Formation (Fig. 6a, b) and in other localities at Wadi El-Yatim conformably overlying the Katkut Formation (Fig. 6c).

The coarse aggregates of the Abu Retag Formation is composed mainly of very coarse-grained gravels intercalated with gravelly sands and sandy beds. These gravelly sediments are predominance of well-rounded particles imbedded in reddish calcareous sand-sized matrix (Fig. 7a) and better-sorted gravelly sized particles (Fig. 7b). Consequently, the basal unit of the Retag Formation exhibits fining-upward mottled and

Table 1 Basic physical and mechanical properties of the studied Oligocene–Pleistocene natural coarse aggregates

Age	Fm.	Site	Sample No.	Grain size characteristics						S_G (gm/cm^3)	Abs.	LAA value (%)
				Gravels %	Sands %	Fines (>0.075 mm) %	C_U	C_C	FM			
Oligocene (?)	Katkut formation	I	1	94.6	4.6	0.8	4.8	3.1	4.5	2.75	0.49	13
			2	95.2	4.4	0.4	5.3	3.4	5	2.76	0.46	14
			3	94.5	4.7	0.8	4.9	3.4	4.8	2.74	0.42	15
			4	94.7	4.6	0.7	4.7	3.3	4.8	2.77	0.45	15
		II	5	95.2	3.9	0.9	4.9	3.4	4.9	2.76	0.44	14
			6	96.1	3.3	0.6	5	3.5	5	2.76	0.46	15
			7	95.3	3.9	0.8	4.6	3.1	4.4	2.75	0.46	14
			8	95.4	4.2	0.4	4.6	3.3	4.8	2.74	0.48	13
			9	95.7	3.8	0.5	4.7	3.4	4.9	2.75	0.48	13
			10	94.8	4.3	0.9	4.9	3.5	4.9	2.72	0.49	14
		III	11	94.5	4.7	0.8	4.9	3.5	5.3	2.75	0.49	15
			12	95.2	4.6	0.2	4.9	3.3	4.9	2.73	0.48	14
			13	94.3	4.2	1.5	4.8	3.5	5	2.76	0.48	15
			14	96.4	2.9	0.7	4.8	3.3	4.8	2.76	0.47	15
		IV	15	95.4	4	0.6	4.8	3.4	5.1	2.76	0.47	14
			16	96.4	3.2	0.4	5	3.6	4.9	2.74	0.47	15
			17	96.6	2.9	0.5	4.7	3.5	5.1	2.76	0.48	16
Average value				95.31	4.01	0.68	4.84	3.38	4.89	2.75	0.47	14.3
Pleistocene	Abbassia formation	V	18	87.7	9.4	2.9	4.6	2.9	4.3	2.68	0.54	19
			19	88.4	8.8	2.8	4.8	2.9	4.5	2.69	0.56	21
			20	87.4	9.8	2.8	4.5	3	4.4	2.67	0.57	22
			21	83.1	13.8	3.1	4.4	3	4.5	2.71	0.58	18
			22	82.1	15	2.9	4.4	2.9	4.4	2.71	0.57	19
			23	81.5	15.3	3.2	4.6	3.1	4.6	2.69	0.58	21
			24	82.4	14.8	2.8	4.4	2.9	4.2	2.69	0.56	20
			25	81.2	15.9	2.9	4.3	3	4.5	2.68	0.59	19
			26	80.2	16.8	3	4.3	3	4.5	2.67	0.56	18
			27	81.1	16.1	2.8	4.4	3	4.4	2.66	0.57	23
		VI	28	82.4	14.8	2.8	4.3	2.9	4.7	2.68	0.55	19
			29	81.2	15.9	2.9	4.5	2.9	4.5	2.69	0.56	18
			30	80.5	16.4	3.1	4.4	3.1	4.6	2.68	0.57	22
		VII	31	81.2	15.9	2.9	4.4	2.9	4.4	2.67	0.58	19
			32	80.4	16.7	2.9	4.3	2.9	4.6	2.67	0.59	18
			33	77.2	19.8	3	4.5	3.1	4.4	2.69	0.57	19
		VIII	34	81.6	15.6	2.8	4.5	2.9	4.6	2.69	0.56	18
			35	80.9	16.1	3	4.5	3.2	4.6	2.69	0.58	21
			36	81.6	15.6	2.8	4.3	2.9	4.5	2.68	0.58	19
			37	80.8	16.4	2.8	4.3	3.2	4.6	2.67	0.58	22
Average value				82.2	14.9	2.9	4.4	2.9	4.45	2.6	0.57	19.7
Pleistocene	Abbassia Fm.	IX	38	93.4	6.4	0.2	4.4	2.7	4.1	2.76	0.47	23
			39	92.8	5.8	1.4	4.3	2.4	4	2.76	0.48	24
			40	92.7	5.7	1.6	4.1	2.6	4	2.75	0.48	23
		X	41	91.5	5.7	2.8	4.1	2.7	4.2	2.75	0.48	22
			42	92.1	5.8	2.1	3.9	2.4	3.9	2.76	0.49	21
			43	92.2	6.4	1.4	4.2	2.7	4.2	2.77	0.49	19
			44	91.8	6.4	1.8	4.2	2.7	4	2.78	0.49	22
		XI	45	91.3	6.7	2	4	2.7	4.2	2.78	0.48	19
			46	91.5	6.7	1.8	3.9	2.6	4.1	2.75	0.46	18
			47	91.7	7.2	1.1	3.9	2.5	3.9	2.75	0.45	21
		XII	48	91.4	7.4	1.2	3.7	2.3	4.1	2.75	0.47	22
			49	92.1	6.3	1.6	4.1	2.5	4.1	2.76	0.48	21
			50	89.8	8.4	1.8	4	2.7	4.2	2.76	0.48	22
Average value				91.9	6.5	1.6	4.1	2.6	4.1	2.76	0.47	21.3

FI (%)	EI (%)	Aggregate shape				Aggregate composition					
		Disc (%)	Blade (%)	Roller (%)	Sphere (%)	Chert (%)	Silicified limestone (%)	Biogenic limestone (%)	Quartz pebbles (%)	Hard limestone (%)	Basement pebbles (%)
18	12	5.7	11.7	26	56.6	81.3	12.6	4.6	1.5	–	–
19	13	5.6	11.6	25.9	56.9	81.6	12.5	4.7	1.2	–	–
21	15	6.1	12.1	26.4	55.4	81.5	12.4	4.5	1.6	–	–
19	14	6	12	26.3	55.7	82.2	11.8	5.1	0.9	–	–
21	15	5.9	11.9	26.2	56	82.3	11.6	5.2	0.9	–	–
20	16	6	12	26.3	55.7	82	12.6	5.2	1.2	–	–
21	14	5.9	11.9	26.2	56	81.8	11.6	5.2	1.4	–	–
20	13	5.9	11.9	26.2	56	81.9	11.4	5.3	1.4	–	–
19	14	6.2	12.2	26.5	55.1	82.3	11.6	5.2	0.9	–	–
21	16	5.7	11.7	26	56.6	81.9	11.8	5.1	1.2	–	–
21	15	5.6	11.6	25.9	56.9	81.4	12.2	4.9	1.5	–	–
20	15	6	12	26.3	55.7	81.6	12	5	1.4	–	–
23	16	5.7	11.7	26.02	56.54	81.2	12.1	5.1	1.6	–	–
22	15	6	12	26.3	55.7	81.4	11.8	5.2	1.6	–	–
21	14	5.9	11.9	26.2	56	81.8	11.4	5.3	1.5	–	–
19	14	5.6	11.6	25.9	56.9	81.8	11.7	5.1	1.4	–	–
21	14	6.1	11.9	23.7	58.3	81.3	11.8	5.3	1.6	–	–
20.3	14.4	5.88	11.8	26.02	56.2	81.7	11.9	5.0	1.34	–	
13	15	2.3	9.7	18.7	69.3	14.3	18.3	58.5	4.5	3.2	1.2
14	15	2.2	9.6	18.6	69.6	14.4	18.4	58.6	4.6	3.3	0.7
15	16	2.7	11.2	19.1	67	14.5	18.5	58.7	4.7	3.4	0.2
13	14	2.6	10	19	68.4	14.4	18.4	58.6	4.6	3.3	0.7
14	15	2.5	10.1	18.9	68.5	14.6	18.6	56.8	4.8	3.5	1.7
13	14	2.6	10.1	19	68.3	14.7	18.7	57.1	4.9	3.6	1
15	15	2.5	9.9	18.9	68.7	14.5	18.5	58.7	4.7	3.4	0.2
14	14	2.5	10.5	18.9	68.1	14.8	18.8	57.5	5	3.7	0.2
14	17	2.8	10.2	19.2	67.8	14.4	18.4	58.6	4.6	3.3	0.7
16	16	2.3	10.2	18.7	68.8	14.4	18.4	58.6	4.6	3.3	0.7
15	17	2.2	9.8	18.6	69.4	14.5	18.5	58.7	4.7	3.4	0.2
14	16	2.6	11.2	19	67.2	14.6	18.6	57.2	4.8	3.5	1.3
14	17	2.32	9.1	18.8	69.78	14.8	18.8	56.7	5	3.7	1
15	15	2.6	11.5	19	66.9	14.3	18.3	58.5	4.5	3.2	1.2
15	16	2.5	10.8	18.9	67.8	14.4	18.4	58.6	4.6	3.3	0.7
14	16	2.2	11.2	18.6	68	14.5	18.5	58.7	4.7	3.4	0.2
14	16	2.3	12.3	18.7	66.7	14.6	18.6	57.1	4.8	3.5	1.4
14	17	2.2	11.2	18.6	68	14.4	18.4	58.6	4.6	3.3	0.7
15	17	2.5	13.4	18.9	65.2	14.7	18.7	57.1	4.9	3.6	1
15	16	2.6	13.2	19	65.2	14.5	18.5	58.7	4.7	3.4	0.2
14.3	15.7	2.4	10.8	18.8	67.9	14.5	18.6	58.1	4.7	3.4	0.7
12	14	1.7	5.6	9.1	83.6	65.4	5.4	4.6	2.1	22.4	0.1
13	11	1.6	5.5	9	83.9	65.1	5.5	4.7	2.2	22.5	0
12	13	2.1	6	9.5	82.4	64.7	5.6	4.8	2.3	22.6	0

14	14	2	5.9	9.4	82.7	65.1	5.5	4.7	2.2	22.5	0
15	13	1.9	5.8	9.3	83	63.9	5.8	5	2.5	22.8	0
12	12	2	5.9	9.4	82.7	63.7	5.8	5	2.5	22.8	0.2
13	14	1.9	5.8	9.3	83	63.8	5.8	5	2.5	22.8	0.1
14	15	1.9	5.8	9.3	83	63.5	5.8	5	2.5	22.8	0.4
13	14	2.2	6.1	9.6	82.1	64.3	5.7	4.9	2.4	22.7	0
12	12	1.7	5.6	9.1	83.6	64.7	5.6	4.8	2.3	22.6	0
14	15	1.6	5.5	9	83.9	63.5	5.9	5.1	2.6	22.9	0
12	15	2	5.9	9.4	82.7	64.9	5.5	4.7	2.2	22.5	0.2
14	12	1.72	5.62	9.12	83.54	64.6	5.6	4.8	2.3	22.6	0.1
13.1	13.3	1.9	5.8	9.3	83	64.6	5.6	4.8	2.3	22.6	0.1

C_U coefficient of uniformity, C_C coefficient of curvature, *FM* fineness modulus, *Abs.* absorption, *LAA* Los Angeles abrasion, *EI* elongation index and *FI* flakiness index

reddish brown gravel-sized cycles (Fig. 7c) separated by paleosol horizons (Fig. 7d). Wedge-like geometry, erosive scour, irregular surfaces, and syndepositional slumping are common (Fig. 7e, f).

The depositional features of the Abu Retag Formation indicated that these sediments were deposited in braided ephemeral channels during high-energy episode of flash floods with confined flows (Miall 1996; Collinson 1996; Mahran et al. 2013). Brookes (1999, 2001) pointed out a presence of wide braided giant flutes, sculptured in Eocene limestone plateaus in the Western Desert of Egypt. The origin of these flutes is related to Miocene catastrophic floods, probably locally caused by erosional and/or tectonic breaching of dams across the Nile Valley drainage.

Consequentially, laminated sand sequence of the Abu Retag Formation suggests temporary playas within a flat alluvial plain. The sheet-like geometry and the absence of stratification of sandstone facies imply unconfined broad channels during high discharge periods (Lee and Chough 1999; Mahran et al. 2013).

The presence of basement pebbles in the Abu Retag Formation indicates that basement in the Western Red Sea Mountains was exposed in Late Miocene and probably extended back to Middle Miocene (Said 1981). The Western Desert of Egypt comprised an ancient W- and NW-flowing river system originating from the Precambrian crystalline rocks of the Red Sea Hills, which were uplifted during the Miocene in association with the opening of the Red Sea. This drainage system is thought to have been active before the onset of the N-flowing Egyptian Nile which started ~6 Ma with the Eonile phase (Roden et al. 2011). As the stratigraphic position of the Abu Retag Formation inter-fingering the upper parts of the Eonile fine siliciclastic of the Nile canyon of Said (1981) during Late Miocene, all given data indicated that the age of the Abu Retag Formation ranges from Middle to Late Miocene time (Mahran et al. 2013).

Pliocene–Quaternary sequence (Paleo-Nile–Neonile)

The Pliocene–Quaternary sequence, belonging to the Paleo-Nile–Neonile stages, forms the Nile terraces between the cultivated flood plains and Eocene limestone cliffs. This sequence is classified into seven lithostratigraphic units; Issawia, Armant, Qena, Abbassia, and Dandara formations.

Issawia Formation

In the studied area, West Sohag, the Issawia Formation (Said 1981) is represented by bedded conglomerates inter-fingering with coarse breccias, accumulated on irregular slope developed on the Eocene rocks. At Wadi El-Yatim, the Issawia Formation crops out plastering the pediments of the western

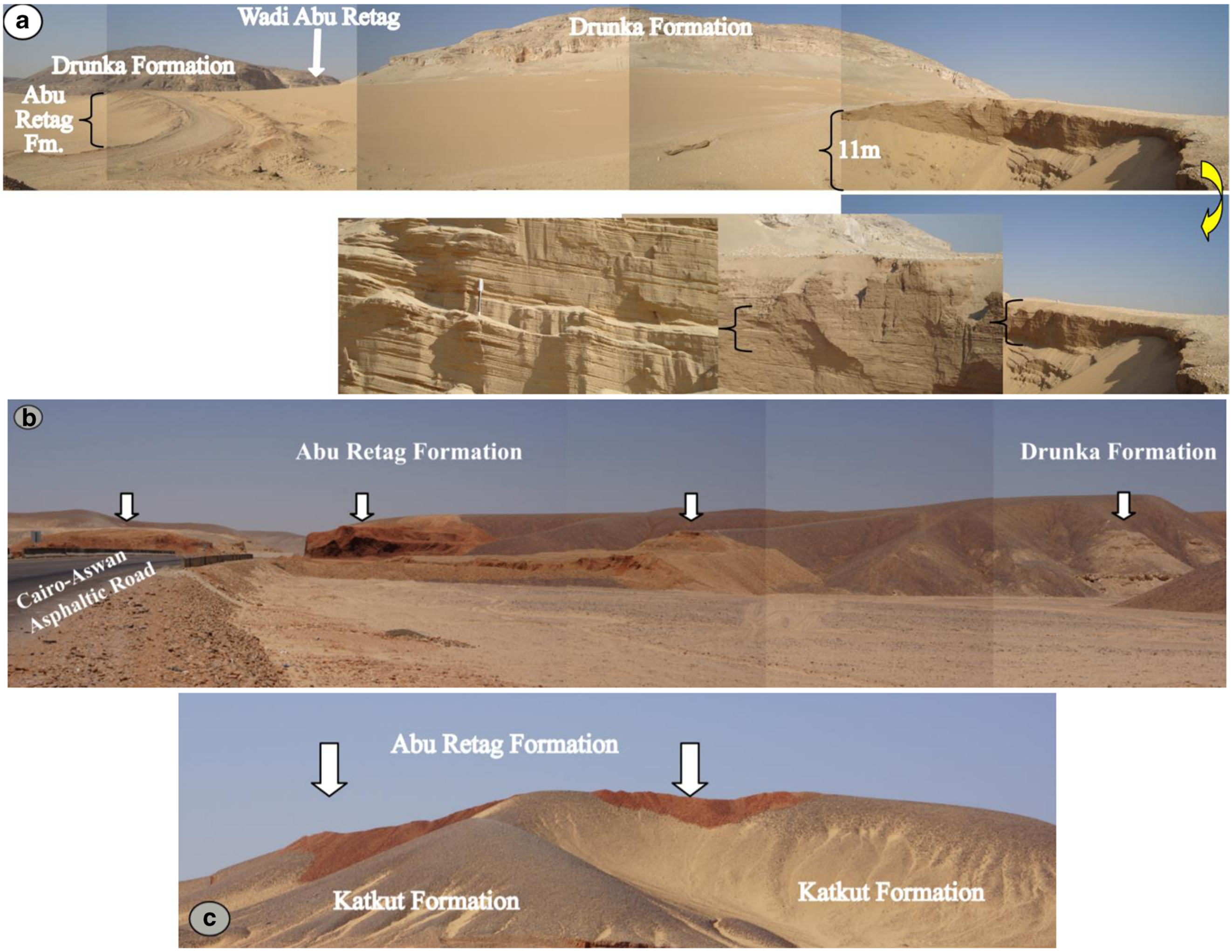

Fig. 6 Field photographs showing Abu Retag Formation unconformably overlies Drunka Formation (**a**, **b**) and conformably overlies Katkut Formation (**c**)

Eocene scarp where it was represented by inclined beds of hard red breccias (up to 15 m thick).

Armant Formation

The Armant Formation (Said 1975; 1981) west of Sohag was dominantly composed of carbonates and tufas (10–20 m thick). At Wadi El-Yatim, it unconformably overlies the Abu Retag Formation and underlies the coarse gravels of the Abbassia Formation (Fig. 1). Both the Issawia and Armant formations are laterally inter-fingering and hence their sediments were contemporaneously deposited (Mahran 1992; Mahran et al. 2013).

Qena Formation

In the study area, the Qena Formation (Said 1981) exhibits low-topographic hills with rounded surfaces and low scarps extending in NW–SE direction near the cultivated land. Many quarries used it as construction fine aggregates. In the northernmost part of the studied area, Qena sands consist of cross-bedded coarse-grained sand cycles followed upward by laminated and cross-laminated fine sands and silts (20 m thick, Abu Seif 2014a).

Abbassia Formation

The Abbassia Formation (Said 1975, 1981) can be easily distinguished in field by its yellowish gray to grayish white coarse aggregates reaching its maximum thickness in areas facing the major wadis draining the Eocene plateaus. The Abbassia Formation conformably overlies and cut-through the Qena Formation (Fig. 8), and in other cases, unconformably overlies the Armant Formation (Fig. 1). In the studied area, west of Sohag, the Abbassia Formation is represented by ~10 m thick (Wadi El-Yatim and Wadi Dukhan, Figs. 1 and 4) of coarsening upward cycles of gravels and sandy gravels. These coarse aggregates (gravels

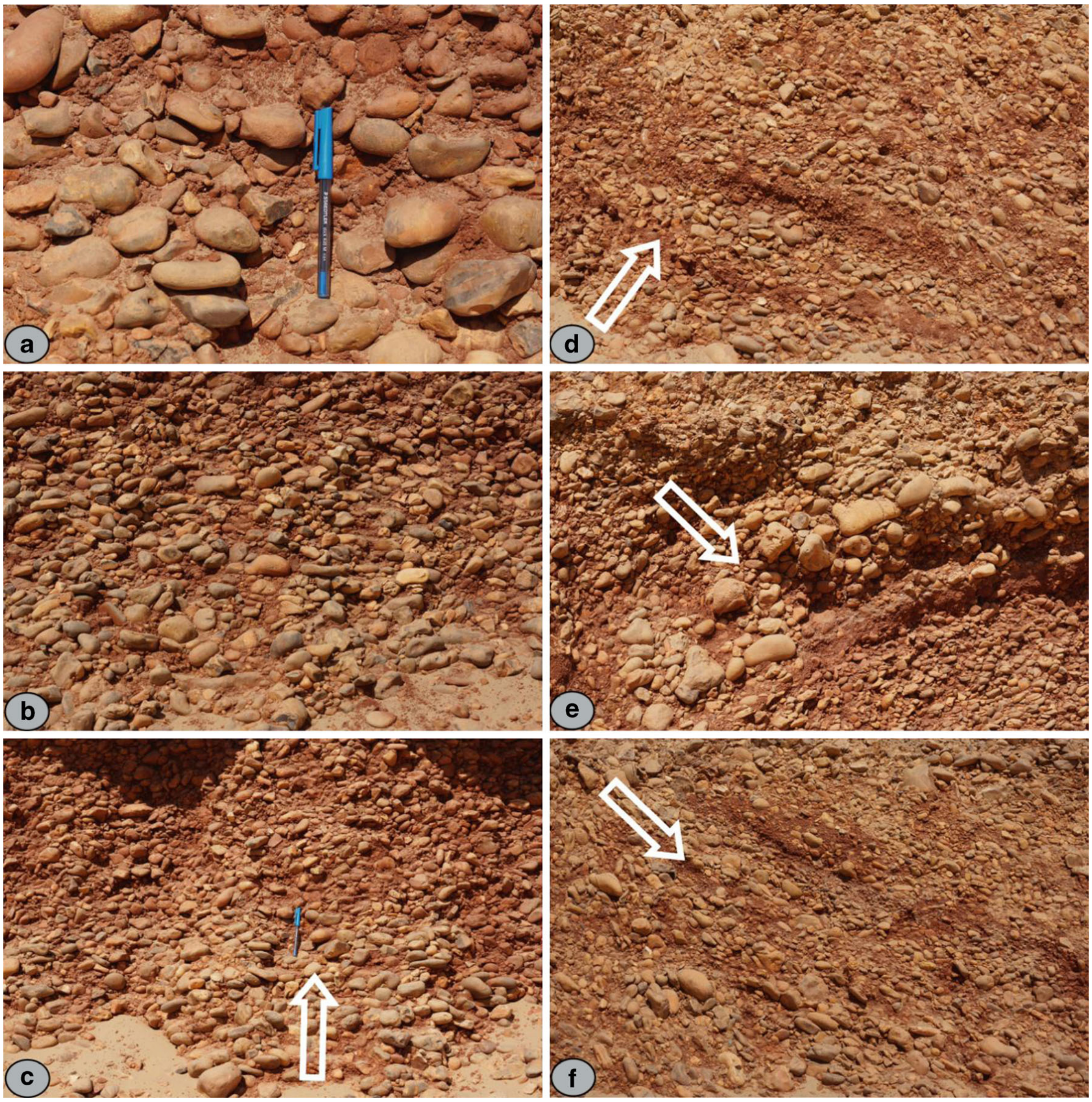

Fig. 7 Field photographs showing some depositional characteristic features of Abu Retag Formation (**a**–**f**)

and sandy gravels) are mostly embedded in a red calcareous sand-sized matrix (Fig. 9). Gravels of the Abbassia Formation are poorly sorted texturally (grain size varies from 2 to 15 cm in diameter) and immature compositionally (chert 64 %, hard limestone 23 %, silicified limestone 6 %, biogenic limestone 5 %, and quartz pebbles 2 % with absence of basement rock fragments; Table 1; Fig. 10). The gravelly lower sequence of the Abbassia Formation followed upward into laminated medium- to fine-grained reddish brown sands sequence, displaying sheet-like geometry. These depositional features indicated that the lower unit of the Abbassia Formation was deposited by debris flow-dominated alluvial fan during high-energy episodic flows of flash floods, whereas the upper unit deposited within alluvial plain (Mahran et al. 2013).

Dandara Formation

The Dandara Formation (Said 1981) forms scattered small hills composed of sands and silt intercalations with lenses of hard sandstones. In the studied area, the Dandara Formation consists of massive silts and fine-grained sands grades upward into gypsiferous clays (3 m thick).

Methodology and practical works

To differentiate between the different rock units in the studied area, intensive field trips, detailed stratigraphic sections, and 15 cross sections were measured and correlated laterally to construct a detailed geological map as well as to understand

Fig. 8 Abbassia Formation conformably overlies natural fine aggregates open cast quarry of Qena Formation (**a**) and coarse-medium-grained cross-bedded sands and laminated fine-grained sands of Qena Formation (**b**, **c**, respectively)

the geological history of the Egyptian Nile in the studied area and its relation with local and regional tectonic events. In the present study, 50 representative samples of natural coarse aggregates were collected from 11 sites (Figs. 1 and 4). The rock

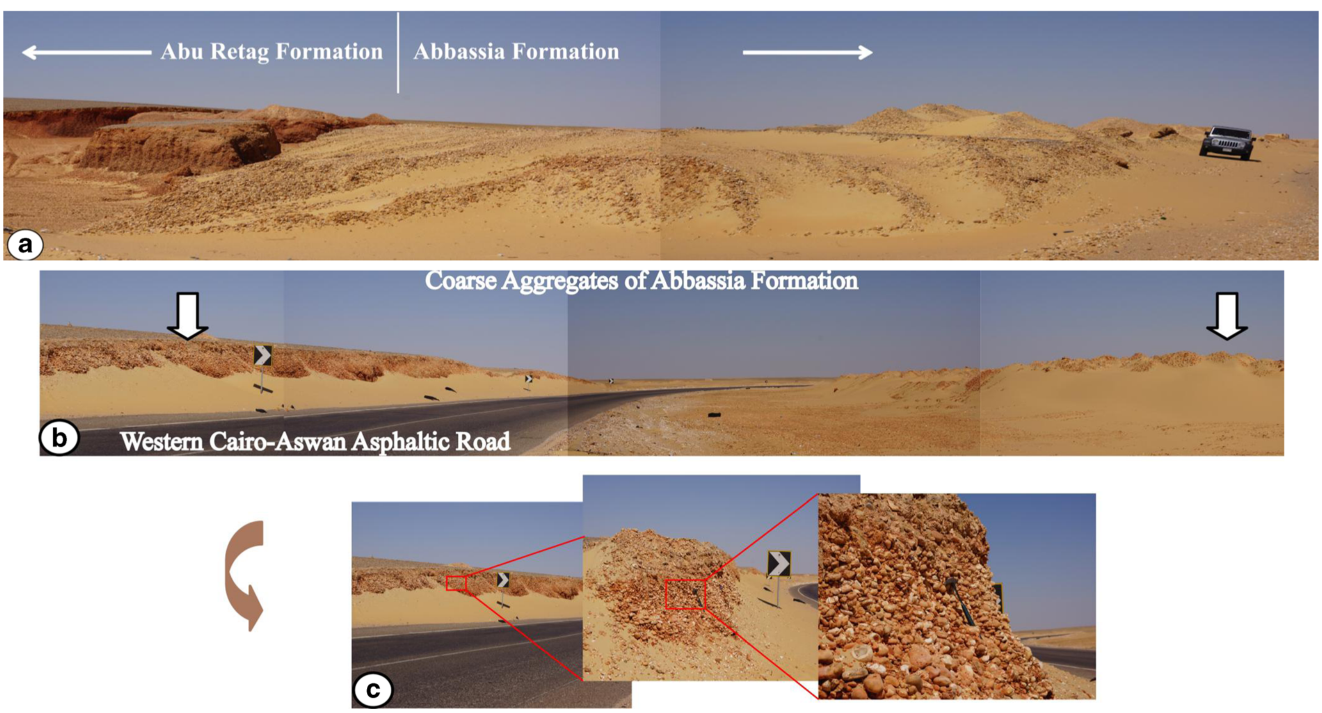

Fig. 9 Field photographs showing Abbassia Formation unconformably overlies natural coarse aggregates of Abu Retag Formation (**a**, **b**) and close-up view of its coarse-grained aggregates (**c**)

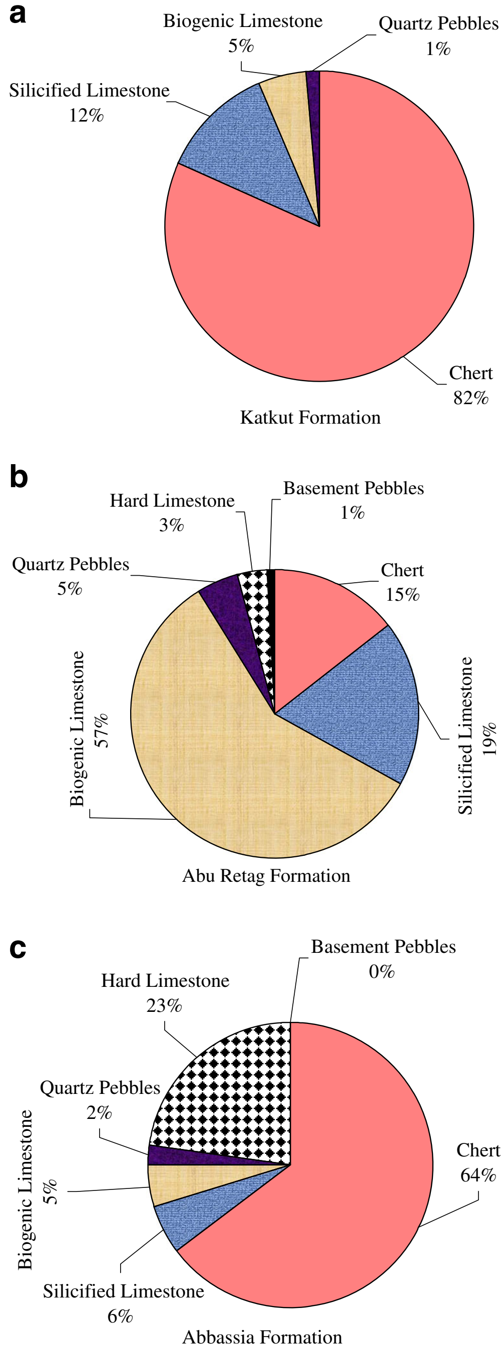

Fig. 10 Pie chart of lithoparticle composition of the studied coarse aggregates (average value)

type of these coarse aggregates was estimated by selecting 100 lithoparticles randomly from each sample and a visual classification was carried out for all of them, according to geological standards. To estimate the shape and textural characteristics of the study aggregates, 100 grains were selected randomly from each representative sample; each grain was classified using Wadell (1932) and Pettijohn (1975) classifications (Table 1). Also, 21 samples representing the different lithostratigraphic units of the studied aggregates in the studied area were subjected to heavy mineral separation (63–125 μm was used for the detailed heavy mineral analysis). Heavy liquid media (Bromoform $CHBr_3$, S_G=2.85) is used to separate heavy minerals. Then heavy mineral grains were mounted on glass slides in Canada Balsam (RI=1.54). Thereafter, 200 grains were point counted along random line traverses in order to determine the opaque/non-opaque ratio. An additional 300 translucent heavy mineral grains were point counted in order to estimate the relative abundance of different mineral species (Table 2). The compositional percentages were determined by using the scheme of Milner (1962) and Tickel (1965).

Also, the studied coarse aggregate samples were subjected to several tests to determine their physical and mechanical properties: sieve analysis (ASTM C 136 2004); specific gravity and absorption (ASTM C127 1999), flakiness index and elongation index (CEN 1997; ASTM D 4791 2005), fineness modulus (ASTM C33 2003), and Los Angeles abrasion value test (ASTM C131 1989).

Results and discussion

The most important geotechnical properties of the aggregates used in road pavements are cleanliness, size and gradation, shape and surface texture, hardness and toughness, durability, and relative density (Tarrer and Wagh 1991; Chen 1995; Chun-Yi and Freeman 1998; Brennan and O'Flaherty 2002; Prowell et al. 2005). The followings are the descriptions and interpretations of the physical and mechanical properties of the studied coarse natural aggregates.

Mineralogical composition

Lithocomposition of Pre-Eonile–Eonile coarse aggregates

The studied area provides a good opportunity for a detailed examination of the effect of source lithology, climate, weathering, transport, and depositional environments on the composition of coarse natural aggregates. Although many studies on modern and ancient sedimentation of the Egyptian Nile Valley have been conducted, major questions concerning compositional relations remain unanswered or were not investigated. Therefore, in the following, the composition framework of the studied aggregates will be identified petrographically to establish provenance of these coarse aggregates. Lithoparticles can often give very specific information on the provenance of a deposit if they can be tied down to a definite area (Tucker 2003). The composition of lithoparticles is considered the best indicators of provenance. It depended basically on source rock, geology, and durability of particles during transportation (Lewis 1984). The studied aggregates

Table 2 Heavy minerals data (63–125 μm) from the studied aggregates converted into percentage values

Age	Fm.	Site	Sample No.	Opaque minerals (%)	Non-opaque minerals (%)									
					Epidote	Pyroxenes	Amphiboles	Zircon	Staurolite	Sphene	Garnet	Apatite	Rutile	Alterites
Oligocene (?)	Katkut Fm.	I	1	25.8	60.9	0	8.4	2.28	0	0.14	0	0	0.08	2.4
			3	22.4	60.7	0	11.72	2.34	0	0.17	0	0	0.09	2.58
		II	8	23.5	60.7	0	10.8	1.9	0	0.1	0	0	0	3
			10	21.4	62.4	0	11.4	2.3	0	0	0	0	0.11	2.39
		III	12	22.4	58.2	0	14.3	2.4	0	0	0	0	0	2.7
			14	21.8	54.5	0	18.7	2.2	0	0	0	0	0	2.8
		IV	17	19.8	61.3	0	13.8	2.17	0	0	0	0	0.13	2.8
Average value				22.44	59.81	0	12.73	2.23	0.00	0.06	0.00	0.00	0.06	2.67
Late Miocene (?)	Abu Retag Fm.	V	21	27.2	37.1	3.6	28.7	1.11	0.13	0.02	0.08	0.07	0.09	1.9
			23	28.7	36	3.8	27.8	1.12	0.11	0.03	0	0.07	0.07	2.3
		VI	28	27.4	37	3.3	28.6	1.15	0.12	0.04	0.07	0.08	0.04	2.2
			30	27.4	35.4	3.4	29.8	1.3	0.13	0.08	0.04	0	0.05	2.4
		VII	32	26.9	34.3	3.5	30.9	1.25	0.18	0.09	0.07	0.08	0.03	2.7
		VIII	35	26.7	37.4	3.3	28.6	1.26	0.18	0.05	0.08	0.07	0.04	2.32
			37	25.8	37.8	3.3	29.2	1.33	0.19	0.08	0.07	0.06	0.07	2.1
Average value				27.16	36.43	3.46	29.09	1.22	0.15	0.06	0.06	0.06	0.06	2.27
Pleistocene	Abbassia Fm.	IX	39	55.76	22.7	11.31	6.1	0.8	0.13	0.11	0.13	0.05	0.11	2.8
		X	41	62.49	18.7	9.8	4.8	0.9	0.18	0.09	0.11	0.09	0.14	2.7
			44	58.4	23.4	10.5	3.9	1.1	0.11	0.07	0.14	0.07	0.11	2.2
		XI	45	54.22	24.7	11.4	5.2	0.8	0.21	0.03	0.11	0.06	0.09	3.18
			47	56.36	25.1	9.2	4.8	0.7	0.23	0.04	0.09	0.08	0.11	3.29
		XII	48	56.6	23.7	10.7	3.9	1.1	0.18	0.05	0.11	0	0.08	3.58
			50	61.02	19.8	9.7	4.2	1.2	0.17	0	0.08	0.08	0.07	3.68
Average value				57.84	22.59	10.37	4.70	0.94	0.17	0.06	0.11	0.06	0.10	3.06

can be subdivided on the basis of lithoparticles framework into three distinct suites as the following:

Suite I (the Katkut Formation, Late Oligocene?) Suite I was distinguished by relative abundance of chert (82 %), silicified limestone (12 %), and biogenic limestone (5 %). This suite is characterized by absence of basement lithoparticles (Table 1; Figs. 10a and 11). The lithoparticles of this suite are characterized by high relative abundance of well-rounded with nearly equi-dimensional particles with absence of basement lithograins; this concluded that the coarse aggregates of the Katkut Formation were derived from the eastern Red Sea Hills, many flowing rivers sourced from the east before being uplifted during Oligocene (El Aref et al. 1987; Kröpelin 1993; Bosworth et al. 2005; Roden et al. 2011; Mahran et al. 2013).

Suite II (Abu Retag Formation, Late Miocene) Suite II coarse aggregates were dominated by relative abundance of biogenic limestone (57 %), silicified limestone (19 %), and chert (15 %). This suite represents the first appearance of basement lithoparticles within Nile Valley sedimentary rock units (Table 1; Figs. 10b and 11). The lithoparticles of the Abu Retag Formation are of mixed basement and carbonate fragments with well-roundness grade referred to the active tectonic uplifting phase of basement shoulders in the eastern Red Sea Hills during Late Miocene–Early Pliocene times (Philobbos et al. 1989). This means that the Abu Retag coarse aggregates are considered an echo of Red Sea rifting during the Late Miocene (Said 1981; Roden et al. 2011; Mahran et. al. 2013).

Suite III (Abbassia Formation, Middle Pleistocene) Suite III coarse aggregates are characterized by dominance of chert (64 %), hard limestone (23 %) silicified limestone (6 %), and biogenic limestone (5 %). This suite is also characterized by absence of basement lithoparticles (Table 1; Fig. 10c).

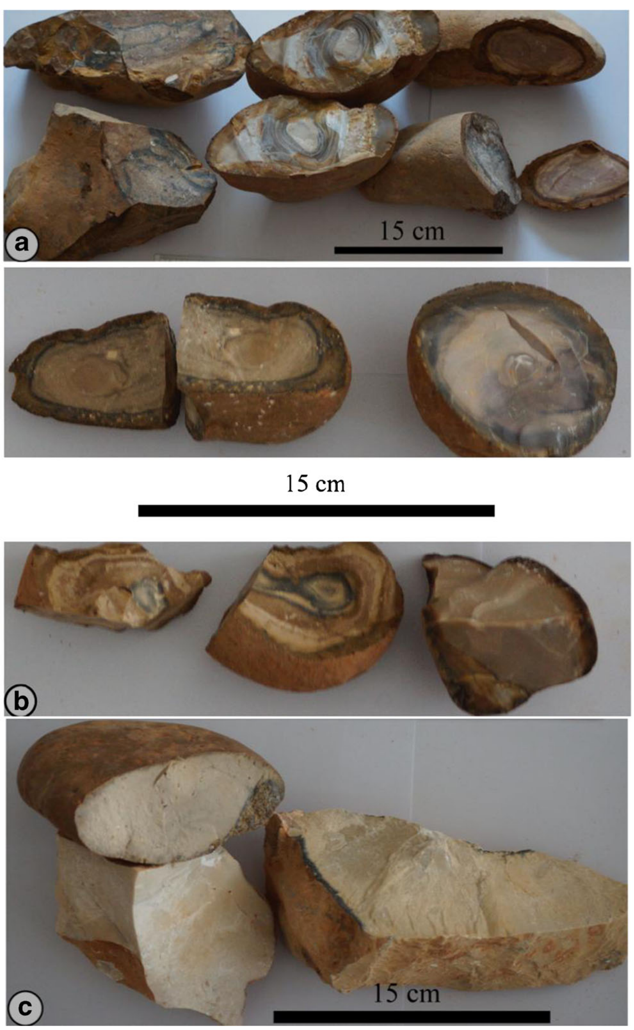

Fig. 11 Photographs of some selected of chert and hard limestone lithoparticles (**a**, **b**) and silicified limestone (**c**)

Heavy mineral analysis of Pre-Eonile–Eonile coarse aggregates

Heavy mineral analysis is one of the most sensitive and widely used techniques in the determination of provenance of clastic sedimentary rocks; heavy mineral data provide constraints on the mineralogical nature of the source terrains. Many of these heavy minerals have very specific and restricted parageneses and therefore provide crucial provenance information that cannot be acquired by any other means (Morton and Hallsworth 1999). Heavy mineral assemblages are affected by three processes, physical sorting, mechanical abrasion, and dissolution (Edelman and Doeglas (1932, 1934).

Minerals of the light fractions consist essentially of quartz grains (mono-crystalline with minor percent of polycrystalline), feldspars (potash and plagioclase feldspars), and carbonate (calcite and microfossil tests). Heavy minerals consist essentially of epidotes, opaques, amphiboles, pyroxenes, alterites, and zircon with trace grains of staurolite, sphene, garnet, rutile, and apatite (Table 2). Epidote is represented by pistachite and zoisite with sub-rounded to rounded grains of green or yellowish to lemon-yellow color varieties. Amphibole was presented by sub-rounded hornblende with minor hypersthene of bluish-green and brownish-green color. Pyroxenes are composed mainly of rounded and well-rounded augite with minor hypersthene grains. Similarly, the studied aggregates can be subdivided on the basis heavy mineral constitutes into three distinct suites (Table 2; Fig. 12) as the following:

Suite I: epidote, opaque and amphibole (Late Oligocene? Katkut Formation) This suite is characterized by dominance of epidotes (60 %), opaques (22 %), and amphiboles (13 %), which are arranged in a decreasing order of abundance with absence of pyroxenes (Fig. 12a). Light fractions

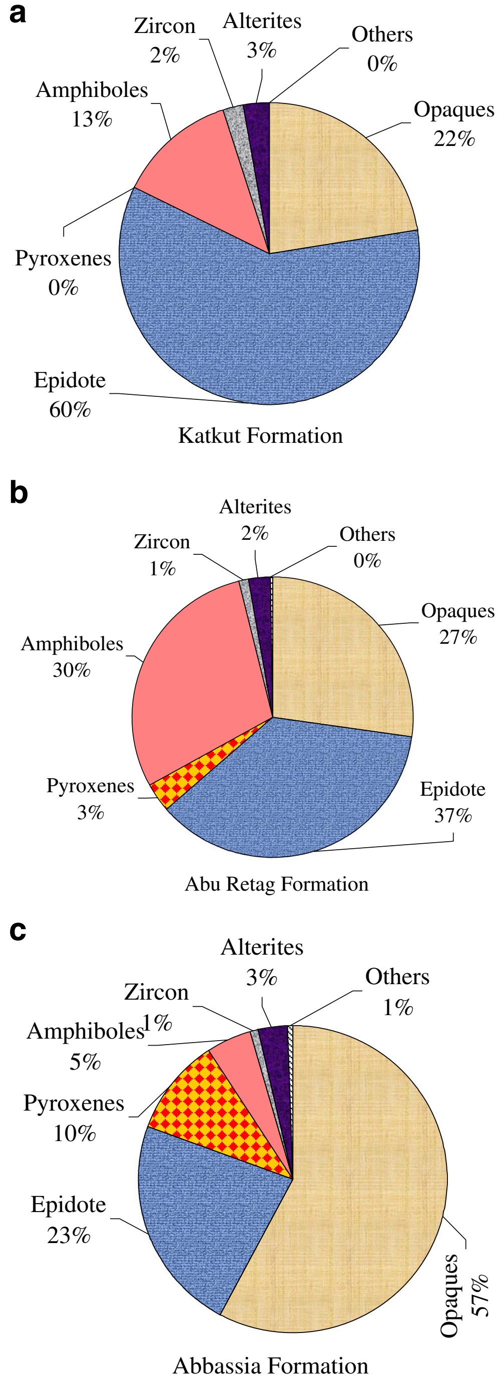

Fig. 12 Heavy mineral assemblages of the studied aggregates (average value)

are composed mainly mono-crystalline quartz grains side limestone and flint rock fragments with the absence of polycrystalline quartz grains.

Suite II: epidote, amphibole, opaque, and pyroxenes (Abu Retag Formation, Late Miocene) This suite is composed mainly of epidotes (37 %), amphiboles (30 %), opaques (27 %), and minor percent of pyroxenes (3 %, Fig. 12b) which arranged in a decreasing order of abundance. It is very important to mention that the light fractions firstly recorded contain basalt and granite rock fragments side-by-side limestone and flint rock fragments. Butzer and Hansen (1968) considered the source of epidote and amphibole to be volcanic and metamorphic rocks. Da Silva (1979) attributed zircon to a granitic provenance. The rounded nature of the heavy mineral grains indicates long distance transportation. This suggests that the source of the Retag Formation is the volcanic and acidic igneous rocks of the basement complex in the Eastern Desert which was uplifted and exposed during Late Miocene (Said 1981; Philobbos et al. 1989; Roden et al. 2011; Mahran et al. 2013).

Suite III: opaque, epidote, pyroxenes, and amphibole (Abbassia Formation, Middle Pleistocene) Suite III consists mainly of opaques (57 %), epidotes (23 %), pyroxenes (10 %), and amphiboles (5 %, Fig. 12c) which is arranged in a decreasing order of abundance. In contrast, abundant pyroxenes characterize the Abbassia Formation (Table 2; Fig. 12c) and mainly consist of rounded augite grains of violet-brown and greenish-yellow colors. In general, pyroxene is usually derived from volcanic rocks. Some grains of pyroxenes are angular, suggesting a short-distance of transport; this angular pyroxene was thus probably derived from exposures of volcanic and meta-volcanic rocks of Red Sea hills (Zaki 2007). However, some authors (Hegab 1989; Mousa 1990; El Asmar and El Fawal 1994) have attributed the assemblages of stable and ferromagnesian minerals in Middle Pleistocene sands at some localities in Egypt to various contributions of Nile sediments and re-sedimentation from basement highs in the Eastern deserts. Also, the high percentage pyroxene of this suite may come from enrichment of pyroxene from underlain the Qena Formation sands by the capture of the Abbassian tributaries (Hegab 1989; El Asmar and El Fawal 1994 and Zaki 2007).

Gradation analysis

Generally, in geotechnical studies that relate to pavement aggregates, gradation curves of both fine and coarse aggregates in determining almost every important property including stability, durability, permeability, workability, and fatigue (Huber and Shuler 1992; Roberts et al. 1996; Prowell et al. 2005; Abu Seif 2014b). The aggregate size and gradation affect the strength, density, and cost of pavements. When particles are bound together by a bituminous binder, a variation in the gradation will change the amount binder needed to produce a mix of given stability and quality (Roberts et al. 1996; Brennan and O'Flaherty 2002). The studied coarse aggregates samples are predominantly with gravels (95 %, 82.2 % and 91.9), sands (4 %, 14.9 and 7 %) and trace amounts of fine materials (silt and clays) around 3 % (0.68 %, 2.9 % and 1.6 %; Table 1; Fig. 13) for the Katkut Formation, Abu Retag Formation, and Abbassia Formation, respectively.

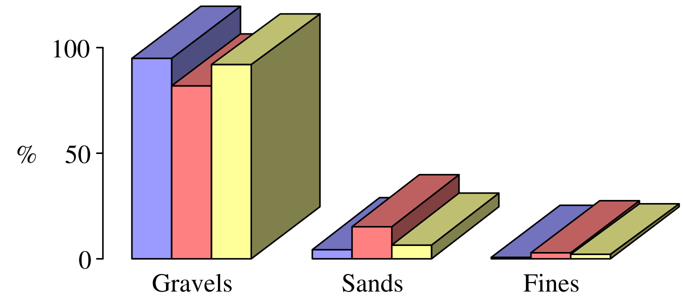

	Gravels	Sands	Fines
Katkut Formation	95.31	4.01	0.68
Abu Retag Formation	82.2	14.9	2.9
Abbassia Formation	91.9	6.5	1.6

Fig. 13 Relative percent of grain size fractions of the studied coarse aggregates (average values)

Figure 14 represents a typical grading chart that showing well-graded distribution for aggregates of the studied coarse aggregates. A well-graded gravel (GW), which contains a wide range of particle sizes, generally producing a compacted layer with high unit weight (low voids), low permeability, and good stability with good distribution of load/stress spreading out uniformly through the material to the road pavement layer below (BS EN 1097-6 2000). In the process of implementing the Superpave system, aggregate characteristics had greater attention than binder materials. Gradation of fineness aggregates affecting more than gradation of coarser aggregates on performance of asphaltic rutting (Kim et al. 2009).

The studied aggregate having smoothed grading curves and neither a deficiency nor excess of any one particle size generally produce a good mixture with fewer voids between particles. A well-graded asphalt mixture exhibits less deformation, well interlocking, high density value, and higher stability (Brown and Pell 1974; Moore and Welke 1979). Within well-graded pavement aggregates, small aggregates submerge in asphalt and the interaction of small aggregates and asphalt follows the so-called parallel mode. Coarser aggregates are glued (coated) together by asphalt and the interaction of coarser aggregates with asphalt follows the so-called serial mode. Therefore, the concept is that small aggregates first “swim” in asphalt to form asphalt mortar and asphalt mortar then coats big aggregates. On the basis of this concept, it is introduced that asphalt pavement here is assumed to be an assembly of asphalt-mortar-coated aggregates (Zhu and Nodes 2000).

According to AASHTO M 147-65 (2004) and ASTM D 1241 (2007), the above-mentioned results indicate that the majority of the studied coarse aggregates met the specified standards limits of gradations which suitable for sub-base course. In the USCS, well-graded gravels must have a C_U value >4 and a C_C value from 1 to 3 is required. The C_U values of the studied aggregates vary from 3.7 to 5.3 and C_C values ranging from 2.3 to 3.3 (Table 1).

The fineness modulus

The fineness modulus (FM) is most commonly computed factor for aggregates. It is used to determine the degree of uniformity of the aggregate gradation. Somewhat, smaller variations in fine aggregate grading can affect the aggregate workability due to the higher surface area. The FM value is an index number which is roughly proportional to the average size of the particles in a given aggregate. The higher the FM,

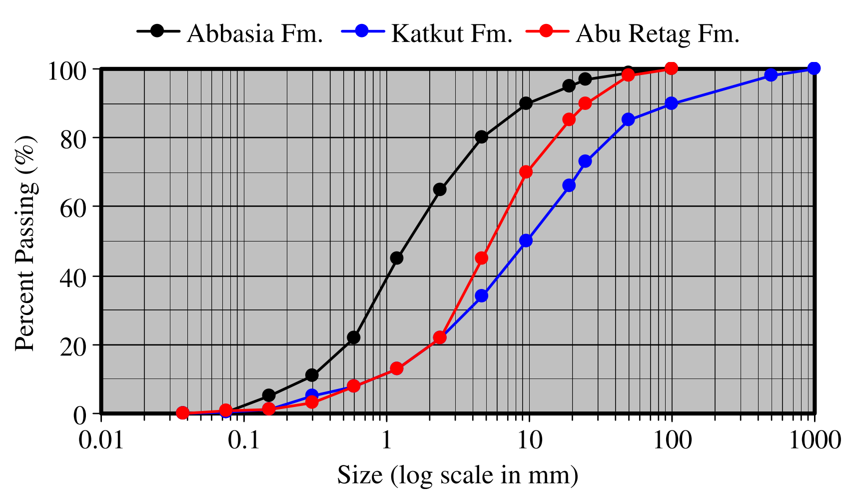

Fig. 14 Grain size distribution curves of the studied coarse aggregates

the coarser the aggregate is. FM values of the studied samples range from 3.9 to 5.3 (Table 1). These results show that the studied aggregates produce pavement with best workability degree and have a highest compressive strength as indicated in ASTM C33 (2003).

Textural characteristics

Shape and roundness degree

From textural characteristics point of view, the particle shape and roundness of pavement aggregates play a vital rule on the workability and strength of the asphalt mix. Irregular or angular particles tend to interlock when compacted and resist displacement. Best interlock is generally obtained with sharp-cornered cubical-shaped particles (Kuo and Freeman 1998; Maerz 2004). Round particles, such as most natural gravels and sands from stream beds, can be used successfully in asphalt paving mixes. Cubical, rough-textured aggregates are more resistant to the shearing action of traffic than rounded, smooth-textured aggregates. Cubical aggregates also tend to interlock better, resulting in a more shear resistant mass of material. In addition, increased compaction during construction or the use of higher percentages of coarse aggregate fractions in the aggregate gradation provides more grain-to-grain contact in the asphalt mix which, in turn, helps to reduce pavement rutting (Imran 2009).

Figure 16 shows detailed investigations of shape and roundness of different lithoparticles of the studied coarse aggregates. The shape of the aggregates directly affects both pavement packing and the way of aggregate particles, forming a skeleton to transmit and distribute traffic loads, thus influencing the stability and mechanical performance of the pavement mixtures (Benson 1970; Marek 1991; Langer and Knepper 1995; Smith and Collis 2001; Shihui and Huanan 2011). Figure 15a shows that the studied aggregates consist mainly of spherical (56.7, 67.9, and 83 %), roller (26.02, 18.8, and 9.3 %), blade (11.8, 10.9, and 5.8 %), and disc (5.88, 2.4, and 1.9 %) shapes, arranged in a decreasing order of abundance for the Katkut Formation, Abu Retag Formation, and Abbassia Formation, respectively. Consequently, these aggregates are having a higher degree of stability and higher wearing resistance (Su 1996; Asphalt Institute, MS-4 2003; Imran 2009; Hamzah et al. 2010).

The result data of roundness degree shows that the studied coarse aggregates are composed mainly of rounded (41, 31 and 25 %), sub-rounded (18, 22 and 28 %), well-rounded (24, 19 and 11 %), sub-angular (9, 15 and 18 %), angular (5, 8 and 11 %) and very angular (3, 5 and 7 %) grains which arranged in a decreasing order of abundance for Katkut Formation, Abu Retag Formation and Abbassia Formation respectively (Fig. 15b). This balanced mixture of roundness degree of the studied coarse aggregates makes considerable shear strength, stability when a load is applied to these aggregates, more grain-to-grain contact with lock tightly together and resistant to rutting of the asphalt mixture (Su 1996; Asphalt Institute MS-4 2003; Imran 2009; Hamzah et al. 2010).

Elongation and flakiness indexes

The flat and elongated aggregate tends to break when subjected to loads, so these types of aggregates are considered undesirable materials in pavement mixtures (Ali and Sengoz 2005). Aggregate particles suitable for use in asphalt roads should be cubical rather than flat, thin, or elongated. The nearly equidimensional grains tend to be more dense and stable under traffic loading and movement. Krutz and Sebaaly (1993) found a direct correlation between the rutting potential of hot mix asphalt mixtures and the shape and texture of coarse aggregate particles. The flakiness (FI) and elongated (EI) indices of the study coarse aggregates were estimated by using flakiness and elongated index gauges. FI values vary from 12 to 23 %, whereas EI values range between 11 and 17 % (Table 1). This means that the studied aggregates of Holocene conglomerates have higher shear strength and exhibit less fatigue life Li and Kett (1967).

Specific gravity

Road aggregates are normally proportioned by mass and, hence, the relative density on an oven-dry basis is of vital importance in determining the proper particle-size blend. Specific gravity of coarse aggregates is essential during the design stage of structural elements and used as well as a useful indicator of the suitability of an aggregate. Specific gravity of aggregate is important for asphalt mix design (Marek 1991). Very low specific gravity frequently indicates aggregate that is porous, weak, or absorptive; heavy weight is used for special purposes such as radiation shielding (Langer 1993).

Specific gravity information about a particular aggregate helps in determining the amount of asphalt needed in the hot mix asphalt. Aggregate specific gravity is useful in making weight-volume conversions and in calculating the void content in compacted hot mix asphalt (Roberts et al. 1996). The specific gravity of aggregates normally used in road construction ranges from about 2.5 to 2.9 (ASTM C127 1999). The specific gravity value of the studied coarse aggregates varies from 2.66 to 2.78 g/cm^3 (Table 1). The narrow variation in specific gravity of the studied aggregates is a very good property in sub-base course applications (Nichols 1991). These results mean that the studied aggregates meet the limits for the coarse aggregate-specific gravity-specified standards.

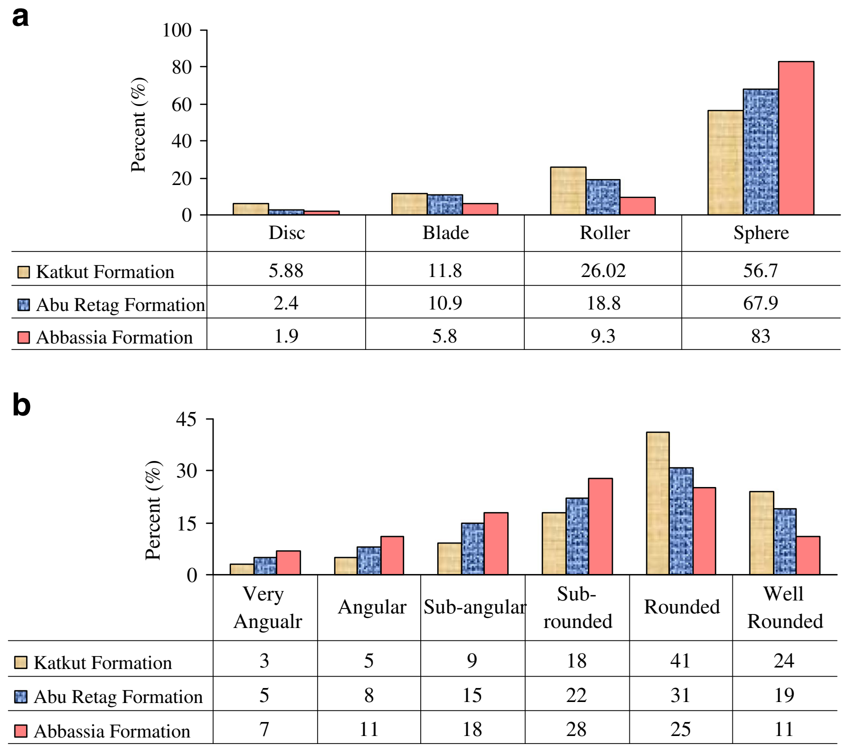

Fig. 15 Particle shape (**a**) and roundness degree (**b**) of the studied aggregates (average value)

Absorption

Aggregates with a high absorption value will absorb greater amounts of the bituminous binder into the aggregate in an asphalt pavement application and thus increase costs. If an aggregate is highly absorptive, the aggregate continues to absorb asphalt, after initial mixing at the plant, until the mix cools down completely. This process leaves less asphalt for bonding purposes; therefore, a more porous aggregate requires more asphalt than a less porous aggregate. Aggregates with high water absorptions (i.e., >2 %) are often considered to be vulnerable to frost action if they are placed in a pavement within 450 mm of the road surface. Water absorption values ranges from 0.1 to about 2.0 % for aggregates normally used in road surfacing (Marek 1991). Absorption value for the studied coarse aggregates ranges from 0.42 to 0.59 (Table 1). These results indicate that the studied aggregates have standard limits for the coarse aggregates absorption-specified standards.

Los Angeles abrasion

Aggregates at or near the pavement surface require greater toughness than aggregate in the lower layers, where loads have dissipated or are not as concentrated. Relatively high resistance

Table 3 Estimated volumes of the studied coarse aggregates

Formation	Site	Total coarse aggregate Estimated volume (million m^3)
Katkut formation	I	430.22
	II	583.10
	III	256.00
	IV	195.55
Abu retag formation	V	128.00
	VI	37.33
	VII	73.95
	VIII	84.62
Abbassia formation	IX	55.47
	X	60.44
	XI	59.73
	XII	96.00
Total volume		2060.41

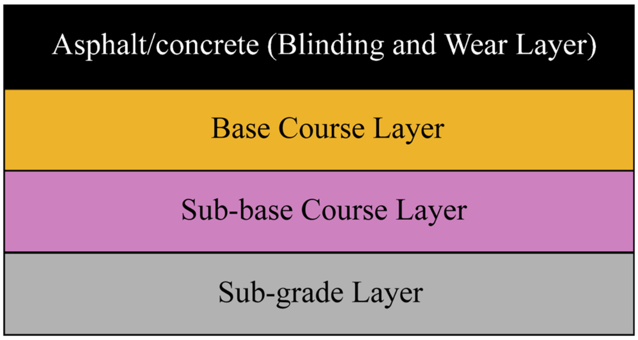

Fig. 16 A typical flexible pavement structure

to wear, as indicted by a low percent of abrasion loss, is a desirable characteristic of aggregates to be used in asphalt pavement surface layers. Aggregates having higher abrasion losses, within limits, may generally be used in lower pavement layers where they will not be subjected to the high stresses caused by traffic. Los Angles abrasion values were determined in the laboratory for coarse aggregates (larger than 2.36 mm) according to ASTM C131 (1989) and are reported in Table 1. The Los Angles abrasion values of the studied coarse aggregates vary from 13 to 24 %. The low Los Angles abrasion values of the studied aggregates indicated a strong coarse aggregate.

Estimation of coarse aggregate potential in the studied area

From an economic point of view, it is very important to assess the potential of these aggregates as volume in cubic meters. Based on the aerial distribution of the mapped coarse aggregate units and their measured thickness in the studied sections (Figs. 1 and 4), the tonnage potentiality is estimated. The total estimated volume is 2060.41 million m^3 (Table 3). These amounts are sufficient for extraction by constructing some quarries. This volume of natural coarse aggregates can be used for road construction after dry sieving processes especially in sub-base course or in base and surface courses after modification their sizes by crushing these aggregates (Fig. 16).

Summary and conclusions

The physical, mineralogical, and mechanical characteristics of the studied natural coarse aggregates of Oligocene–Pleistocene sequence, west Sohag Governorate, Upper Egypt were compared with the international standards of pavement aggregates. Consequently, the main conclusions of this study are as follows:

1. There are several factors affecting the lithotype and distribution of the Post-Eocene sedimentary rock units in the Egyptian Nile Valley; regional tectonics, local structures, and climatic changes.
2. The rock type, mineral composition, and textural characteristics of Oligocene–Pleistocene natural coarse aggregates, west Sohag Governorate, Upper Egypt, have been reflected six distinct stages of Nile Valley geological evolution.
3. A significant interaction between the gradation, shape angularity, composition, dry density, absorption, and abrasion resistance of the aggregate was recorded.
4. From the physical and mechanical characterization point of views, the Oligocene–Pleistocene aggregate sequences are properly suitable for materials to be used in the sub-base of pavement.
5. These coarse natural aggregates can be naturally dry sieved and crushed to use as base and surface courses aggregates.
6. The estimated reserve of these coarse aggregates (west Sohag Governorate, Upper Egypt) covers more than 2060.41 million m^3.

Acknowledgments The author is deeply grateful to Prof. Dr. A.M. Al-Amri (the Editor-in-Chief) and the anonymous reviewers for insightful comments and criticism that improved the original manuscript.

References

AASHTO M 147-65 (2004) Standard specification for materials for aggregate and soil-aggregate subbase, base, and surface courses. American Association of State and Highway Transportation Officials/4 pages

Abdel Hamid MA, Abdel Kawy WA, Ali RR, Ibrahim RA (2014) Study of land resources of some areas at Helwan Governorate. Int J Environ Sci 3(1):27–35

Abdel Razzik TM (1972) Comparative studies on the upper Cretaceous-Early Paleocene sediments on the Red Sea coast, Nile Valley and Western Desert Egypt, 8th Arab Petroleum Congress, Algiers, paper No. 71(B-3), 1–23

Abu Seif ES (2014a) Geotechnical approach to evaluate natural fine aggregates concrete strength, Sohag Governorate, Upper Egypt. Arab J Geosci. doi:10.1007/s12517-014-1705-3

Abu Seif ES (2014b) Geomechanical evaluation of Pliocene natural aggregates as pavement materials. Arab J Geosci 7:1567–1576

Akawy A (2002) Structural geomorphology and neotectonics of the Qina; Safaja District, Egypt. Neues Jahrbuch fuer Geologie und Palaeontologie 226:95–130

Akbulut H, G rer C (2007) Use of aggregates produced from marble quarry waste in asphalt pavements. J Build Environ 42:1921–1930

Akkad S, Dardir AA (1966) Geology of the Red Sea coast between Ras Ghagara and Mersa Alam. Egypt Geol Surv, 35–67

Ali T, Sengoz B (2005) Determination of fine aggregate angularity in relation with the resistance to rutting of hot-mix asphalt. Constr Build Mater 19:155–163

Amoroso S, Leopardi M, Totani G (2008) From geotechnical and hydraulic researches to use of natural materials in mitigation works for river embankments: a case study

Asphalt Institute MS-4 (2003) Superpave mix design. Superpave Series SP-2, 3rd Edition, Lexington, Kentucky, USA

ASTM C127 (1999) Standard Test Method for Specific Gravity and Absorption of Coarse Aggregate. Annual Book of ASTM Standards, 4.02, American Society for Testing and Materials, Philadelphia, 64–68

ASTM C131 (1989) Method for resistance to degradation of small size coarse aggregate by abrasion and impact in Los Angles machine, ASTM C131, Philadelphia

ASTM C136 (2004) Standard Test Method for Sieve Analysis of Fine and Coarse Aggregates, ASTM Annual Book of Standards, Vol. 04–02

ASTM C33 (2003) Standard specification for concrete aggregates. American Society for Testing and Materials, ASTM specification, Philadelphia

ASTM D1241 (2007) Specification for materials for soil-aggregate sub-base, base and surface courses. American Society for Testing and Materials

ASTM D4791 (2005) Standard test method for flat particles, elongated particles, or flat and elongated particles in coarse aggregate, ASTM, West Conshohocken

Barron T (1907) The Topography and Geology of the District between Cairo and Suez. Egyptian Survey Department, 1–133

Beadnell HJL (1905) The Topography and Geology of the Fayum Province of Egypt. Survey Department, 1–101

Benson FJ (1970) Effects of aggregate size shape, and surface texture on the properties of bituminous mixtures—a literature survey. Highway Res Spec Rep 109:12–21

Blair TC, McPhersonb JG (1994) Historical adjustments by Walker River to lake-level fall over a tectonically tilted half-graben floor, Walker Lake Basin, Nevada. Sed Geo 92(1–2):7–16

Bosworth W, Huchon P, McClay K (2005) The Red Sea and Gulf of Aden Basins. J Afr Earth Sci 43:334–378

Bown TM, Kraus MJ (1988) Geology and paleoenvironment of the Oligocene Jebel Qatrani Formation and adjacent rocks, Fayum Depression, Egypt: U.S. Geol Surv Prof Pap 1452:1–60

Brennan MJ, O'Flaherty CA (2002) Highways. 4th edition, Elsevier Ltd. ISBN: 978-0-7506-5090-8

Brookes IA (1999) Geomorphic maps of Egypt's Western Desert. Abstracts XV Congress International Association for Quaternary Research (INQUA), Durban, South Africa, 33

Brookes IA (2001) Possible Miocene catastrophic flooding in Egypt's western desert. J Afr Earth Sc 32:325–333

Brown SF, Pell PS (1974) Repeated loading of bituminous materials. CAPSA 74. National Institute for Road Research, Republic of South Africa, Durban

BS EN 1097-6 (2000) Tests for mechanical and physical properties of aggregates: Part 6: Determination of particle density and water absorption

Butzer KW (1959) Contributions to the Pleistocene geology of the Nile Valley. Erdkunde 13:46–67

Butzer KW, Hansen CL (1968) Desert and River in Nubia. Wisconsin University press, Madison, **562p**

CEN, European Committee for Standardization (1997) EN 933-3. Tests for general properties of aggregates: part 3, determination of particle shape, Flakiness index, Brussels

Chen WF (1995) The civil engineering handbook. CRC Press, Florida

Chun-Yi K, Freeman RB (1998) Image analysis evaluation of aggregates for asphalt concrete mixtures. Transp Res 1615:65–71

Collinson JD (1996) Alluvial sediments. Sediment Environ: Process Facies Stratigraph 3:37–82

Conoco (1987) The Egyptian general petroleum corporation, geological map of Egypt 1: 500,000

Da Silva M (1979) Provenance of heavy minerals in beach sand, south eastern Brazil; from Rio Grande to Chui (Rio Grande do sul state). Sed Geo 24:133–149

Dec T (1992) Textural characteristics and interpretation of second-cycle, debris-flow-dominated alluvial fans (Devonian of Northern Scotland). Sed Geo 77(3–4):269–296

Edelman CH, Doeglas DJ (1932) Reliktstructuren detritischer pyroxene und amphibole. Tschermaks Mineral Petrogr Mitt 42:482–490

Edelman CH, Doeglas DJ (1934) Über umwandlungserscheinungen an detritischem staurolith und anderen mineralien. Tschermaks Mineral Petrogr Mitt 44:225–234

El Aref MM, Abou Khadrah AM, Lotfy ZH (1987) Karst topography and karstification processes in the Eocene limestone plateau of El Bahariya Oasis, Western Desert, Egypt. Zeitschrift fur Geomorphologie, NF 31(1):45–64

El Asmar H, El Fawal F (1994) Depositional history of prenile, west of the Delta, Egypt and its correlation with eastern Mediterranean stratigraphy. Sedimentol Egypt 2:41–53

El-Bastawesy M, Faid A, Gammal ESE (2010) The Quaternary development of tributary channels to the Nile River at Kom Ombo area, Eastern Desert of Egypt, and their implication for groundwater resources. Hydrol Process 24:1856–1865

Goudie AS (2005) The drainage of Africa since the Cretaceous. Geomorphology 67:437–456

Hadlari T, Rainbird RH, Donaldsan R (2006) Alluvial, eolian and lacustrine sedimentology of a paleopreterozoic half-graben, Baker lake basin, Nunavut, Canada. Sed Geo 190:47–70

Hamzah MO, Puzi MAA, Khairun Azizi AM (2010) Properties of geometrically cubical aggregates and its mixture design. IJRRAS 3(3): 249–256

Hegab O (1989) Old Nile alluvium in Upper Egypt. Bull Fac Sci El Mansoura Univ Egypt 16:73–94

Hoggs SE (1982) Sheet-floods, sheet wash, sheet flow. Earth Sci Rev 18: 59–76

Huber GA, Shuler TS (1992) Providing sufficient void space for asphalt cement: Relationship of mineral aggregate voids and aggregate gradation, ASTM SPT 1147, Philadelphia, PA

Imran H (2009) Impact of hot mix asphalt properties on its permanent deformation behaviour. Ph D. thesis, Civil Engineering Department, Faculty of Civil and Environmental Engineering, University of Civil Engineering and Technology, Taxila, Pakistan

Issawi B (2005) Archean-Phanerozoic birth and the development of the Egyptian Land. 1st Int. In Conf. on Geol. Tethys, Cairo University, 339–380

Issawi B, McCauley JF (1992) The Cenozoic Rivers of Egypt; the Nile problem. In: Friedman R, Adams B (eds) The followers of Horus. Oxford Monograph, Oxford, pp 121–138

Issawi B, McCauley JF (1993) The Cenozoic landscape of Egypt and its river systems. Egypt Geol Surv 19:357–384

Issawi B, Osman R (2008) Egypt during the Cenozoic: geological history of the Nile River. Bull Tethys Geol Soc Cairo 3:43–62

Issawi B, El-Hinnawi M, Francis M, Mazhar A (1999) The Phanerozoic geology of Egypt—a geodynamic approach. The Egyptian Geological Survey Press, Cairo, **462p**

Kim YR, Park MH, Aragâo STF, Lutif SEJ (2009) Effects of aggregate structure on hot-mix asphalt rutting performance in low traffic volume local pavements. Constr Build Mater 23:2177–2182

Krijgsman W, Hilgen FJ, Raffi I, Sierro FJ, Wilson DS (1999) Chronology, causes and progression of the Messinian salinity crisis. Nature 400:652–655

Kröpelin S (1993) Geomorphology, landscape evolution and paleoclimates of Southwest Egypt. Catena Suppl 26:31–65

Krutz NC, Sebaaly PE (1993) Effect of aggregate gradation on permanent deformation of asphaltic concrete. Proc Assoc Asphalt Paving Technol 62:450–473

Kuo C-Y, Freeman RB (1998) Image analysis evaluation of aggregates for asphalt concrete mixtures, Transport Res Rec, No. 1615, TRB, National Research Council, Washington, D. C., 65–71

Langer WH (1993) Natural aggregates of the conterminous United States. US Geol Surv No. 1594, 2nd Printing

Langer WH, Knepper DHJr (1995) Geologic characterization of natural aggregate: a field geologist's guide to natural aggregate resource assessment: US Geol Sur Open-File Report 95–582, 32p

Lee S, Chough S (1999) Changes in sedimentary facies and strata patterns along the strike-slip margin, northeastern Jinan Basin (Cretaceous), southwest Korea, implications for differential subsidence. Sediment Geol 128:81–102

Lewis DW (1984) Practical Sedimentology. Hutchinson Ross, Stroudsburg, PA, **229p**

Li MC, Kett I (1967) Influence of coarse aggregate shape on the strength of asphalt concrete mixtures. Highw Res Rec 178:93–106

Maerz NH (2004) Technical and computational aspects of the measurement of aggregate shape by digital image analysis. J Comput Civil Eng ASCE 18:10–18

Mahran TM (1992) Sedimentological development of the Upper Pliocene-Pleistocene sediments in the area of El Salamony and El Sawamha Sharq, NE Sohag, Nile Valley, Egypt. Sohng Pure App Sci Bull Fac Sci Assiut Univ Egypt 8:251–276

Mahran TM (1997) Cyclicity in Nakheil formation (Oligocene), West of Quseir, Red Sea, Egypt. Egypt J Geol 42(2A):309–546

Mahran TM (1999) Late Oligocene lacustrine deposition of the Sodmin Formation, Abu Hammad Basin, Red Sea. Egypt: sedimentology and factors controlling palustrine carbonates. J Afr Earth Sc 29(3): 567–592

Mahran TM, El-Shater A, Youssef AM, El-Haddad BA (2013) Facies analysis and tectonic-climatic controls of the development of Pre-Eonile and Eonile sediments of the Egyptian Nile west of Sohag. The 7th international conference on the geology of Africa, Assiut, Egypt, (Abstract)

Mandanici E, Bitelli G, Curzi PV (2010) Hyper and multispectral image analysis in north-eastern Libyan Desert. Hyperspectral Workshop, Frascati, Italy, 17–19th March, ESA SP-683

Marek CR (1991) Basic properties of aggregate. In: Barksdale RD (ed) The aggregate handbook, Ch. 3. National Stone Association, Washington, D.C, pp 1–81

McCauley J, Breed C, Schaber G (1986) The megageomorphology of the radar rivers of the eastern Sahara. JPL Second Spaceborne Imaging Radar Symposium, 25–36

McCauley JF, Schaber GG, Breed CS, Grolier MJ, Haynes CV, Issawi B, Elachi C, Blom R (1982) Subsurface valleys and geoarcheology of the Eastern Sahara revealed by Shuttle Radar. Science 218:1004–1020

Miall AD (1996) The geology of fluvial deposits: sedimentary facies, basin analysis and petroleum geology. Springer, Berlin, **582p**

Milner HB (1962) Sedimentary petrography, part II. Principals and applications. Macmillan, New York, 715p

Moore RB, Welke RA (1979) Effects of fine aggregate on stability of bituminous mixes, research report No. 78 TB-34-79F, Testing Laboratory Section, Testing Research Division, Michigan Department of Transportation, Lansing, MI

Morton AC, Hallsworth CR (1999) Processes controlling the composition of heavy mineral assemblages in sandstones. Sediment Geol 124:3–29

Mousa B (1990) Petrology and soil genesis of the surface Quaternary deposits, east of the Nile Delta. Ph.D. thesis, Faculty of Science, Ain Shams University, Egypt, 391p

Nichols FP (1991) Specifications, standards, and guidelines for aggregate base course and pavement construction. In: Barksdale RD (ed) The aggregate handbook: National Stone Association, Washington, D.C. 1–33

Omar GI, Steckler MS (1995) Fission track evidence on the initial rifting of the Red Sea: two pulses, no propagation. Science 270:1341–1344

Omran AA (2008) Integration of Remote Sensing, Geophysics and GIS to Evaluate Groundwater Potentiality: A Case Study in Sohag Region, Egypt. The 3rd International Conference on Water Resources and Arid Environments and the 1st Arab Water Forum

Pettijohn FJ (1975) Sedimentary rocks. Harper and Raw Publisher, Inc., New York, **638p**

Philobbos ER, El-Haddad AA, Mahran TM (1989) Sedimentology of the syn-rift Upper Miocene (?)-Pliocene sediments of the Red Sea areas: a model from the environs of Marsa Alam. Egypt J Geol 33:210–226

Prowell BD, Zhang J, Brown ER (2005) NCHRP Report 539 Aggregate properties and the performance of Superpave-designed hot mix asphalt, Transport Res Board, Washington, D.C

Roberts FL, Kandhal PS, Brown ER, Lee D-Y, Kennedy TW (1996) Hot mix asphalt materials, mixture design and construction, 2nd ed. Lanham, MD, NAPA Research and Education Foundation

Roden J, Abdelsalam MG, Atekwana E, El-Qady G, Tarabees EA (2011) Structural influence on the evolution of the pre-Eonile drainage system of southern Egypt: insights from magnetotelluric and gravity data. J Afr Earth Sc 61:358–368

Said R (1962) The geology of Egypt. Elsevier, Amsterdam-New York, **377p**

Said R (1975) The geological evolution of the River Nile. In: Wendorf F, Maks AF (eds) Problems in Prehistory of Northern Africa and the Levant. Southern Methodist University Press, Dallas, pp 1–44

Said R (1981) The geological evolution of the River Nile. Springer, New York

Said R (1983) Proposed classification of the Quaternary of Egypt. J Afr Earth Sc 1:41–45

Said R (1990) The Geology of Egypt. S.A., Balkema, Rotterdam, Brookfield, 731p

Said R (1992) The geology of Egypt. Elsevier Science Ltd, Rotterdam

Said R (1993) The River Nile: geology, hydrology and utilization. Pergamon Press, Oxford, **320p**

Shihui S, Huanan Y (2011) Characterize packing of aggregate particles for paving materials: particle size impact. J Construc Build Mater 3: 1362–1368

Shukri NM (1954) On cylindrical structures and coloration of Gebel Ahmar near Cairo, Egypt. Bull Fac Sci Cairo Univ 32:1–23

Shukri NM, Ayouty MK (1954) The mineralogy of Eocene and later sediments in the Anqabia Area, Cairo-Suez District. Bull Fac Sci Cairo Univ No 32:47–61

Smith MR, Collis L (2001) Aggregates–sand, gravel and crushed rock aggregates for construction purposes (3rd edition). Geol Soc London, Chapter 8:199–224

Su Z (1996) Mineral aggregates; their classifications and properties, ESHA Research Report, RT010-96-02, Department of Research and Technology, Smid & Holland Services B.V

Tarrer AR, Wagh V (1991) The effect of the physical and chemical characteristics of the aggregate on bonding. Strategic Highway Research Program, National Research Council, Washington, D.C

Thurmond AK, Stern RJ, Abdelsalam MG, Nielsen KC, Abdeen MM, Hinz E (2004) The Nubian swell. J Afr Earth Sc 39:401–407

Tickel FG (1965) The techniques of sedimentary mineralogy. Elsevier, Amsterdam, **220p**

Tucker ME (2003) Sedimentary rocks in the field, 3rd edition. John Wiley & Sons Ltd, 250p

Wadell H (1932) Volume, shape and roundness of rock particles. J Geol 40:443–451

Wendorf F, Schild R (1976) Prehistory of the Nile Valley. Academic, New York, p 404

Zaki R (2007) Pleistocene evolution of the Nile Valley in northern Upper Egypt. Quat Sci Rev 26:2883–2896

Zhu H, Nodes JE (2000) Contact based analysis of asphalt pavement with the effect of aggregate angularity. Mech Mater 32:193–202